Eur. Phys. J. C 50, 949–968 (2007)
DOI 10.1140/epjc/s10052-007-0238-2

THE EUROPEAN PHYSICAL JOURNAL C

Regular Article – Theoretical Physics

Dark matter and collider searches in the MSSM

Y. Mambrini[1,2,a], E. Nezri[3]

[1] Laboratoire de Physique Théorique des Hautes Energies, Université Paris-Sud, Orsay, France
[2] Deutsches Elektronen-Synchrotron DESY, Notkestrasse 85, 22607 Hamburg, Germany
[3] Service de Physique Théorique, Université Libre de Bruxelles, 1050 Brussels, Belgium

Received: 28 July 2005 / Revised version: 28 September 2006 /
Published online: 20 March 2007 –

Abstract. We study the complementarity between dark matter experiments (direct detection and indirect detection) and accelerator experiments (the CERN LHC and a $\sqrt{s} = 1\,\text{TeV}$ e^+e^- linear collider) within the framework of the constrained minimal supersymmetric standard model (MSSM). We show how non-universality in the scalar and gaugino sectors can affect the experimental prospects to discover the supersymmetric particles. The future experiments will explore a large part of the parameter space of the MSSM favored by the Wilkinson Microwave Anisotropy Probe (WMAP) constraint on the relic density, but there still exist some regions beyond reach for certain extreme (fine tuned) values of the supersymmetric parameters. Whereas the focus point region characterized by heavy scalars will be easily probed by experiments searching for dark matter, the regions with heavy gauginos and light sfermions will be accessible more easily by collider experiments. More information on both supersymmetry and astrophysics parameters can thus be obtained by combining the different signals.

1 Introduction

Numerous independent astrophysical and cosmological measurements suggest that the matter in our universe is dominated by a not yet identified dark component (see e.g. [1–4] for reviews). The solution of this problem is crucial to the understanding of our universe. The missing matter has been probed by a variety of experiments on different scales of astrophysics, such as galaxy observations through rotation curves, clusters through X-ray emission and on the cosmological scale through CMB anisotropy measurements. The CMB data provides the most stringent constraint and gives the total fraction of dark matter in the universe with the best accuracy. Indeed, the recent WMAP [5,6] results lead to a flat concordance model universe with a relic density of cold dark matter of

$$\Omega_{\text{CDM}}h^2 = 0.1126^{+0.0161}_{-0.0181} \quad \text{at} \quad 95\%\,\text{CL}\,. \tag{1}$$

The accuracy of the measurement is expected to increase with future data from the PLANCK satellite [7] and a precision of $\Delta\Omega_{\text{CDM}}h^2 \sim 2\%$ has been projected.

An interesting possibility for such a cold dark matter candidate is a bath of long lived or stable weakly-interacting massive particles (WIMPs) left over from the Big Bang in sufficient numbers to account for their observed relic density. Since additional constraints, especially those from light element nucleosynthesis, strongly disfavor the possibility that dark matter is composed solely of baryons [8], some form of "non-standard" matter is required.

The standard model (SM) of high energy physics, despite its success in explaining the data available today, requires an extension to explain the hierarchy between the weak and the Planck scales, the unification of gauge couplings and the origin of electroweak symmetry breaking. The most popular extension of the model is the minimal supersymmetric standard model (MSSM) [9–12]. The MSSM predicts the existence of several new particles, namely the superpartners of the SM ones. In most of the MSSM parameter space, the lightest supersymmetric particle (LSP) is a stable, massive, neutral, weakly-interacting particle: the lightest neutralino. This stable particle offers an interesting and well motivated dark matter candidate. On the other hand, at future colliders such as the Large Hadron Collider (LHC) and the planned International Linear e^+e^- Collider (ILC), supersymmetric particles are expected to be produced and observed if low energy supersymmetry (SUSY) is present in nature. However, even if part of the supersymmetric spectrum is unveiled at the LHC, for example, the properties of the particles that play a dominant role in the relic density will not be measured directly or precisely. Both types of data (from astroparticle as well as from accelerator physics) are thus needed to extract the full properties of the underlying supersymmetric model [13].

In constrained MSSM, such as the minimal supergravity model (mSUGRA), the minimization of the one-loop scalar potential leads to the well-known relation between the squares of the superpotential Higgs mass term and the

[a] e-mail: mambrini@th.u-psud.fr

soft-SUSY breaking scalar Higgs masses m_{H_u}, m_{H_d} as well as the ratio of the vacuum expectation values of the two Higgs fields, $\tan\beta = v_d/v_u$, and the Z-boson mass M_Z. The relation

$$\mu^2 = \frac{\left(m_{H_d}^2 + \delta m_{H_d}^2\right) - \left(m_{H_u}^2 + \delta m_{H_u}^2\right)\tan^2\beta}{\tan^2\beta - 1} - \frac{1}{2}M_Z^2 \tag{2}$$

is imposed at the SUSY breaking scale, defined as the geometric average of the two top squark masses, $M_{\rm SUSY} = \sqrt{m_{\tilde{t}_1} m_{\tilde{t}_2}}$. This condition determines the absolute value of the term μ, leaving its sign as a free parameter of the theory.

The four neutralinos ($\chi_1^0 \equiv \chi, \chi_2^0, \chi_3^0, \chi_4^0$) are superpositions of the neutral fermionic partners of the electroweak gauge bosons $\widetilde{B}^0$ and $\widetilde{W}_3^0$ (respectively the B-ino and W-ino fields) and the superpartners of the neutral Higgs bosons $\tilde{H}_u^0$, $\tilde{H}_d^0$ (respectively the up and down higgsino fields). In the $(\widetilde{B}, \widetilde{W}^3, \widetilde{H}_d^0, \widetilde{H}_u^0)$ basis, the neutralino mass matrix is given by

$$\mathcal{M}_N = \begin{pmatrix} M_1 & 0 & -m_Z\cos\beta\sin\theta_W & m_Z\sin\beta\sin\theta_W \\ 0 & M_2 & m_Z\cos\beta\cos\theta_W & -m_Z\sin\beta\cos\theta_W \\ -m_Z\cos\beta\sin\theta_W & m_Z\cos\beta\cos\theta_W & 0 & -\mu \\ m_Z\sin\beta\sin\theta_W & -m_Z\sin\beta\cos\theta_W & -\mu & 0 \end{pmatrix}, \tag{3}$$

where M_1, M_2 are the bino and wino mass parameters, respectively. This matrix can be diagonalized using an orthogonal matrix z, and we can express the LSP χ (often referred to in the following as the neutralino) as the linear combination

$$\chi = z_{11}\widetilde{B} + z_{12}\widetilde{W} + z_{13}\widetilde{H}_d + z_{14}\widetilde{H}_u\,. \tag{4}$$

The eigenvector components determine the nature, couplings and phenomenology of the neutralino. The neutralino is usually called "gaugino-like" if $P \equiv |z_{11}|^2 + |z_{12}|^2 > 0.9$, "higgsino-like" if $P < 0.1$, and "mixed" otherwise.

An annihilation rate consistent with the WMAP constraint can be obtained by several mechanisms, depending on the model parameters: when $m_\chi \approx m_{\tilde{\tau}_1}$ bino-$\chi\tilde{\tau}$ coannihilation dominates; for large tanβ values or a light pseudoscalar A-boson, $\chi\chi \xrightarrow{A} b\bar{b}$ annihilation is dominant; for a sufficiently higgsino-like neutralino, $\chi\chi \to t\bar{t}$ dominates. At the same time, a non-negligible wino component can enhance the annihilation process $\chi\chi \to W^+W^-$ and the $\chi\chi^\pm$ and $\chi^+\chi^-$ coannihilation processes.

In the present work, we will consider neutralino dark matter searches in direct or indirect detection experiments and the prospects of superparticle production at future colliders like LHC or ILC, working within the framework of general supergravity scenarios with non-universal scalar and gaugino soft-SUSY breaking mass terms.

The outline of the paper is as follows. Section 2 summarizes the phenomenology of the various dark matter searches. Section 3 discusses the prospects for producing and detecting SUSY particles and MSSM Higgs bosons at the LHC and at a high energy e^+e^- collider. Section 4 presents a complementary analysis for each type of signal and the influence of non-universality on the detection prospects of all types of experiments. For our computation, we use an interface of the latest released version of the SUSPECT codes [14] for the MSSM particle spectrum, MICROMEGAS [15, 16] for the neutralino relic density, and DARKSUSY [17] for the dark matter detection rates. During the writing of this paper, the authors of [18] and [19] carried out a similar analysis and reached conclusions in agreement with those presented here. Related work in a variety of frameworks and dealing with cosmological relic density aspects, present accelerators constraints and/or dark matter searches and/or SUSY searches at future colliders can be found in [20–66].

2 Dark matter searches

2.1 Dark matter distribution

The dark matter distribution within the galaxy is a crucial ingredient for many detection techniques. From N-body simulations, this distribution is commonly parameterized as

$$\rho(r) = \frac{\rho_0[1 + (R_0/a)^\alpha]^{(\beta-\gamma)/\alpha}}{(r/R_0)^\gamma[1 + (r/a)^\alpha]^{(\beta-\gamma)/\alpha}}\,, \tag{5}$$

where r is the galacto-centric coordinate, ρ_0 is the local (i.e. in the neighborhood of the Sun) halo density, R_0 the solar distance to the galactic center and a a characteristic length. While there is agreement concerning the predicted behavior at large radii ($\beta \sim 3$), the exponent describing the possible cusp at the center is the subject of discrepancies between various groups carrying out numerical simulations ($1 \lesssim \gamma \lesssim 1.5$). Furthermore, studies of low surface brightness galaxies seem to favor flat cores. Moreover, the central region behavior may depend strongly on the physical assumptions regarding baryonic effects on the central dark matter density, supermassive black hole induced spikes, dark matter particles scattering on stars, etc. (For a discussion, see e.g. [67–72].) Finally, possible inhomogeneities and substructures could be present, leading to possible clumpiness of the halo.

In contrast, there is general agreement on the local density ρ_0 that can be determined for each density profile assuming compatibility with the measurements of the rotational curves and the total mass of the galaxy; ρ_0 should range from 0.2 to 0.8 GeV cm^{-3} (see [2] for a discussion). For definiteness, our results are presented for $\rho_0 = 0.3$ GeV cm^{-3} for all the density profiles used in the present analysis. A more controversial topic is the possible link between the dark matter distribution and the total relic abundance. One can rescale the density $\rho(r)$, when the calculated value of $\Omega_\chi h^2$ is smaller than the WMAP lower bound, by assuming that

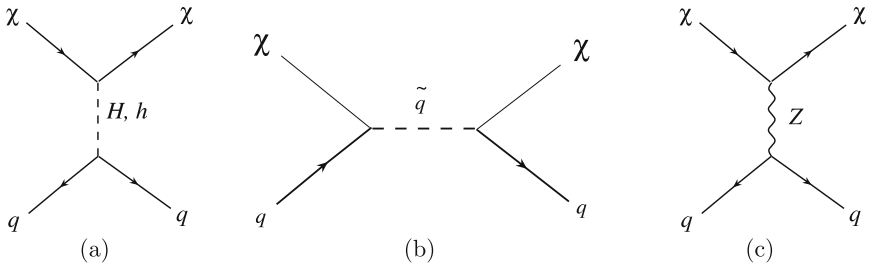

Fig. 1. Feynman diagrams of the processes occurring in direct detection of the lightest neutralinos: **a** and **b** spin independent processes ($\sigma_{\chi p}^{\rm scal}$); **b** and **c** spin dependent processes ($\sigma_{\chi p}^{\rm spin}$)

the neutralino could form only a fraction of the total amount of cold dark matter. In this study, however, we will not use this procedure as we will mainly focus on the dependence of the detection rates on the SUSY parameter space for a given astrophysical framework.

2.2 Direct detection

Many underground experiments have been carried out around the world in order to detect WIMP candidates by means of their elastic scattering off target nuclei through nuclear recoil [73]. As previously pointed out, the astrophysical uncertainties in the predicted rate for this type of detection technique is small. Namely, the translation of the detection rates/sensitivities to the scattering cross section $\sigma_{\chi p}$ relies only on knowledge of the local dark matter density ρ_0. Depending on the spin of the target nuclei, the detection rate is given by the spin dependent ($\sigma_{\chi p}^{\rm spin}$) or the spin independent ($\sigma_{\chi p}^{\rm scal}$) neutralino–nucleon elastic cross section. The main contributing diagrams are shown in Fig. 1.

The squark exchange contributions (mainly the first generation $\tilde{u}$, $\tilde{d}$ squarks) are usually suppressed by the squark masses. The spin independent cross section $\sigma_{\chi p}^{\rm scal}$ is then driven by neutral CP-even Higgs boson (h, H) exchanges ($\chi q \xrightarrow{h,H} \chi q \propto z_{11(2)} z_{13(4)}$) and the spin dependent cross section $\sigma_{\chi p}^{\rm spin}$ by Z-boson exchange ($\chi q \xrightarrow{Z,} \chi q \propto z_{13(4)}^2$). Direct detection is thus more favored for a mixed gaugino–higgsino neutralino and models where the scalar Higgs boson H is sufficiently light.

In the usual mSUGRA scenario, where the soft terms of the MSSM are assumed to be universal at the unification scale, the spin independent cross section is constrained by $\sigma_{\chi p}^{\rm scal} \lesssim 3 \times 10^{-8}$ pb[1]. However, it has been shown that if the assumption of universality in the scalar and/or gaugino sectors is relaxed, the cross section can be increased significantly compared to the universal scenario and could reach values of the order $\sigma_{\chi p}^{\rm scal} \sim 10^{-6}$ pb [31–35]. QCD corrections to the neutralino–nucleon scattering cross sections may also be relevant [74].

Current experiments such as EDELWEISS [75] and CDMS [76, 77] are sensitive to WIMP–proton cross sections larger than approximately 10^{-6} pb, excluding the DAMA region [78]. These sensitivities are slightly too small to probe minimal SUSY models if we impose the accelerator constraints and the bound on the relic density from WMAP. Several new or upgraded direct WIMP detection experiments will soon reach a significantly improved sensitivity (GENIUS, EDELWEISS II [79], ZEPLIN(s) [80], CDMS II and superCDMS [81]). The next generation of experiments (e.g. EDELWEISS II and CDMS II) will lead to a minimum of the valley sensitivity around 10^{-8} pb for a neutralino mass of $m_\chi = \mathcal{O}(100\,\text{GeV})$. Though challenging from the experimental point of view, a ton size detector (ZEPLIN, SuperCDMS) should be able to reach $\sigma_{\chi p}^{\rm scal} \gtrsim 10^{-10}$ pb. In our study, we will take the neutralino mass dependent projected experiment sensitivities of EDELWEISS II [79] and ZEPLIN [80].

2.3 Indirect gamma detection

Dark matter can also be observed through its annihilation products in the galactic halo. In particular, the annihilation at the galactic center (GC), where the dark matter density is important, could lead to large fluxes and promising experimental signals even if the exact behavior in the central region is poorly constrained. Unfortunately, the astrophysical uncertainties dominate largely over the ones coming from particle physics models, considerably affecting the discovery prospects of indirect gamma detection experiments.

The main annihilation processes entering in the calculation of gamma-ray fluxes from the GC are depicted in Fig. 2. The large masses of the scalar fermions and their small Yukawa couplings usually suppress the contribution of the diagrams with t-channel sfermions exchange. The dominant cross sections are thus $\sigma\big(\chi\chi \xrightarrow{A} b\bar{b}\big) \propto \big[z_{11(2)} z_{13(4)}\big]^2$, $\sigma\big(\chi\chi \xrightarrow{Z} t\bar{t}\big) \propto \big[z_{13(4)}^2\big]^2$ and $\sigma\big(\chi\chi \xrightarrow{x^+(\chi_j^0)} W^+W^-(ZZ)\big) \propto \big[z_{13(4)} V_{12}\big]^2$ and/or $\big[z_{12} V_{11}\big]^2$ $\big(\big[z_{13(4)} z_{j3(4)}\big]^2\big)$, with $V_{\rm ij}$ the chargino mixing matrices. Annihilation in these channels is favored for a wino-like and a higgsino-like neutralino. The resulting observed differential gamma-ray flux at the Earth coming from a direction forming an angle ψ with respect to the GC is

$$\frac{\mathrm{d}\Phi_\gamma(E_\gamma,\psi)}{\mathrm{d}\Omega\,\mathrm{d}E} = \sum_i \frac{1}{2}\frac{\mathrm{d}N_\gamma^i}{\mathrm{d}E_\gamma}\langle\sigma_i v\rangle \frac{1}{4\pi m_\chi^2} \times \int_{\text{line of sight}} \rho^2\left(r(l,\psi)\right)\mathrm{d}l\,, \tag{6}$$

[1] For a recent review, see [4].

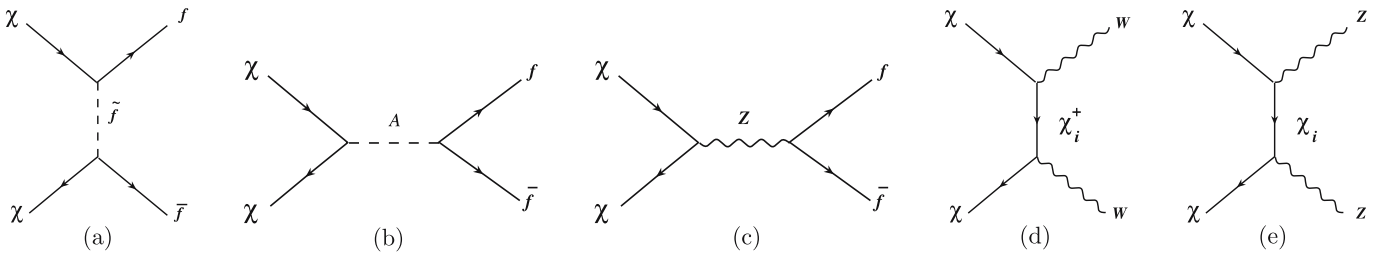

Fig. 2. Feynman diagrams for the dominant channels contributing to neutralino annihilation into SM particles

where the discrete sum is over all dark matter annihilation channels, $\mathrm{d}N_\gamma^i/\mathrm{d}E_\gamma$ is the differential gamma-ray yield and $\langle\sigma_i v\rangle$ is the annihilation cross section averaged over the velocity distribution. It is customary to isolate the dependence on the halo dark matter model with respect to particle physics, defining the dimensionless quantity [82, 83]

$$\bar{J}\left(\Delta\Omega\right) = \frac{1}{8.5\,\mathrm{kpc}}\left(\frac{1}{0.3\,\mathrm{GeV/cm^3}}\right)^2 \times \int_{\Delta\Omega}\int_{\text{line of sight}} \rho^2\left(r(l,\psi)\right)\,\mathrm{d}l\,\mathrm{d}\Omega \qquad (7)$$

over a solid angle $\Delta\Omega$ centered on $\psi = 0$.

As pointed out, a crucial ingredient for the calculation of the annihilation fluxes is the density profile of dark matter around the core of the GC. In the present work, we choose the intermediate Navarro, Frenk and White (NFW) halo profile [84] ($\gamma = 1$, $\bar{J}_{\mathrm{NFW}}(\Delta\Omega = 10^{-3}) \sim 10^3$). One can rescale the fluxes to have results for other commonly used profiles either with a stronger cusp like the one proposed by Moore et al. [85] ($\gamma = 1.5$, $\bar{J}_{\mathrm{Moore}}(\Delta\Omega = 10^{-3}) \sim 10^5$) or a shallower slope like the one proposed by Kravtsov et al. [86] ($\gamma = 0.4$, $\bar{J}_{\mathrm{Kravtsov}}(\Delta\Omega = 10^{-3}) \sim 10$).[2] The sensitivity to such variations in the dark matter profile of the experimental prospects will be illustrated later; see 10c and d. In the literature, some authors [83] also consider as a theoretical input parameter a boost factor acting on $\bar{J}$, to account for possible halo inhomogeneities (from clumps for instance).

Recently several experiments have detected a significant gamma-ray flux from near the galactic center. Observations by INTEGRAL [87] and EGRET [88, 89] have revealed γ-ray emission from this region, although no corresponding sources have been identified so far. The VERITAS [90] and CANGAROO [91] collaborations using, respectively, the Whipple 10 meters and CANGAROO-II atmospheric Cerenkov Telescopes (ACTs) have independently detected TeV γ-rays from the same region. Finally, HESS [92] claims to have observed a signal corresponding to a WIMP in the multi-TeV energy range. Here we refrain from interpreting all these signals as due to dark matter annihilation. Although an explanation in terms of a heavy dark matter particle like the LSP neutralino [59, 60, 92] is possible for each signal (except for INTEGRAL; see for instance [93] for a light dark matter scenario proposal), these measurements are not compatible with each other and cannot be explained by a single scenario. Moreover, purely astrophysical interpretations of these signals are possible [94, 95].

In any case, considering the computational uncertainties and the existence of alternative astrophysical explanations [94, 95], it is reasonable not to attribute these signals to a neutralino and proceed with our analysis of constraints on the SUSY parameter space attainable from future experiments. Nevertheless, the EGRET signal ($\sim 4\times10^{-8}\,\gamma\,\mathrm{cm^{-2}\,s^{-1}}$) can be seen as an upper bound even if one has to keep in mind that it may not arise exactly from the galactic center [96]. We will also consider the sensitivities of the HESS [97] and GLAST [98] experiments (respectively, $10^{-12}\,\gamma\,\mathrm{cm^{-2}\,s^{-1}}$ with a 100 GeV threshold and $10^{-10}\,\gamma\,\mathrm{cm^{-2}\,s^{-1}}$ with a 1 GeV threshold) as a probing test of our models. The neutralino mass dependent integrated sensitivities used in our analysis can be found in [99].

2.4 Indirect neutrino detection

Dark matter particles of the halo can also be trapped in astrophysical bodies (like the Sun) by successive elastic scattering off its nuclei (hydrogen) over the age of the target object ($\sim 10^{10}$ years). This leads to a captured population which annihilates, producing neutrino fluxes that can be detected by a neutrino telescope, manifesting the presence of dark matter. The direction of the neutrino can be used to distinguish such flux from a diffuse background noise. The annihilation rate at a given time t can be written as [100–102]

$$\Gamma_{\mathrm{A}} = \frac{1}{2}C_{\mathrm{A}}N_\chi^2 = \frac{C}{2}\tanh^2\sqrt{CC_{\mathrm{A}}}t\,, \qquad (8)$$

where C is the capture rate, which depends on the local density ρ_0 and on the neutralino–proton elastic cross section. $\Gamma_{\mathrm{A}} \approx \frac{C}{2} = \text{constant}$ when the neutralino population has reached equilibrium, and $\Gamma_{\mathrm{A}} \approx \frac{1}{2}C^2C_{\mathrm{A}}t^2$ during the initial collection period. When accretion is efficient, the annihilation rate follows the capture rate C and thus the neutralino-quark elastic cross section, whereas only the differential spectrum depends on the annihilation processes. The flux is then given by

$$\frac{\mathrm{d}\Phi_\nu}{\mathrm{d}E_\nu} = \frac{\Gamma_{\mathrm{A}}}{4\pi R^2}\sum_F B_F\frac{\mathrm{d}N_\nu^F}{\mathrm{d}E_\nu}(E_\nu)\,, \qquad (9)$$

[2] For $\gamma \geq 1.5$, $\bar{J}$ diverges and one has to regularize the integral of (1).

where F labels the annihilation final states and R is the Sun–Earth distance. As related to the local dark matter density, the astrophysical dependence is weak, and similarly in the direct detection case. One should note that the neutralino capture rate is time dependent. The trapped population could have been larger in the past if the Sun traversed some clumps of dark matter.

The particle physics behavior is dominated by the capture rate driven by $\sigma_{\chi p}$. The dominant processes are shown on Fig. 1 (spin dependent for the Sun because of the non-zero hydrogen nuclear spin). The couplings have already been described in the section on direct detection. The dominant diagrams describing annihilation (see Fig. 2) and their couplings have been discussed in the section devoted to indirect gamma detection. For our analysis we will consider the fluxes coming from the Sun, which is favored for neutralinos with a non-negligible higgsino component. Indeed Z exchange is then allowed in neutralino–quark diffusion and the resulting flux can be high. The annihilation may also enhance the flux, especially by giving harder neutrino spectra when the higgsino and/or the wino fraction are not negligible leading to $t\bar{t}, W^+W^-$ final states instead of $b\bar{b}$ for a dominant bino neutralino [32, 103].

The Earth could be another possible source, but the resulting fluxes are beyond the reach of detection [103]. The neutralino annihilations in the galactic center can also lead to neutrino fluxes ($i = \nu$ in (7)), but the gamma flux is much more promising given the experimental sensitivities [104].

Present experiments like MACRO [105], BAKSAN [106], SUPER K [107] and AMANDA [108] (whose size and location disfavor detection of horizontal fluxes from the Sun) limit the possible fluxes to around $10^4 \mu\,\mathrm{km}^{-2}\,\mathrm{yr}^{-1}$. Future neutrino telescopes like ANTARES [109] or a km^3 size like ICECUBE [110] will be able to probe respectively around 10^3 and $10^2 \mathrm{m}\,\mathrm{km}^{-2}\,\mathrm{yr}^{-1}$. We used the neutralino mass dependent sensitivities of [111] for ANTARES and [112] for ICECUBE.

2.5 Indirect positron detection

Neutralino annihilations in the halo can also give rise to measurable positron fluxes. Being charged particles, positrons interact during their propagation so that directional information is lost. Furthermore, these interactions imply that the observed positrons do not originate from far away in the galaxy. In addition to the variability of the density profiles, which is a source of uncertainties at their production, the understanding of the propagation taking into account interactions with magnetic fields and inverse Compton and synchrotron processes is the most relevant and difficult question to control in order to be able to understand their fluxes and to estimate the positron spectra. The positron flux results from the steady state solutions of the diffusion-loss equation for the space density of cosmic rays per unit energy, $\mathrm{d}n/\mathrm{d}\varepsilon$:

$$\frac{\partial}{\partial t}\frac{\mathrm{d}n}{\mathrm{d}\varepsilon} = \nabla\cdot\left[K(\varepsilon,x)\nabla\frac{\mathrm{d}n}{\mathrm{d}\varepsilon}\right] + \frac{\partial}{\partial\varepsilon}\left[b(\varepsilon,x)\frac{\mathrm{d}n}{\mathrm{d}\varepsilon}\right] + Q(\varepsilon,x) = 0\,, \qquad (10)$$

where K is the diffusion constant (assumed spatially constant throughout a "diffusion zone", but possibly energy dependent), b the energy loss rate and Q the source term (see [50] for details). We take [113]

$$K(\varepsilon) = 3.3\times10^{28}\left[3^{0.47}+\varepsilon^{0.47}\right]\mathrm{cm}^2\,\mathrm{s}^{-1} \qquad (11)$$

and [114]

$$b(\varepsilon)_{e^+} = 10^{-16}\varepsilon^2\mathrm{s}^{-1}\,, \qquad (12)$$

which results from inverse Compton scattering off both the cosmic microwave background and diffuse starlight. The diffusion zone is a slab of thickness $2L$ ($L = 4\,\mathrm{kpc}$ to fit observations of the cosmic ray flux, see [47] and references therein). Variations of the propagation parameters may change the results of the computation by around an order of magnitude [51]. The source term $Q = f(\rho(r), \langle\sigma v\rangle)$ can be modified if one considers the presence of clumps in the (quite local) dark matter distribution and a possible resulting multiplicative boost factor $b \lesssim 10$ [52]. The particle physics dependence also enters in the source term and comes from the supersymmetric parameter influence on the annihilation cross section (see Fig. 2 and Sect. 2.3).

The HEAT experiment (consisting of three flights in 1994, 1995 and 2000), observed a flux of cosmic positrons in excess of the predicted rate, peaking around10 GeV [115]. This signal may be explained by neutralino annihilation but requires a boost factor [51, 53]. Furthermore, the HEAT measurement uncertainties in the 30 GeV bin are quite large. Consequently, we estimate here the fluxes for the future experiments AMS-02 and PAMELA. The exact positron spectrum depends on annihilation final states, dark matter distribution and propagation parameters [51], but as a reasonable approximation for our analysis one may assume that the spectra are peaked at around $M_\chi/2$. At those energies, we have checked that the background of [116] can be fitted by $E^2\,\mathrm{d}\Phi_{e^+}/\,\mathrm{d}\Omega\,\mathrm{d}E \simeq 1.16\times E^{-1.23}$. Following [26, 66], we require as a condition for the detection $\frac{\phi^{e^+}_\chi}{\phi^{e^+}_{\mathrm{Bckgd}}}|_{m_\chi/2} \sim 0.01$ (see [18] for more precise criteria).

2.6 Indirect antiproton detection

Another possible signal of dark matter may be the detection of antiproton fluxes produced by neutralino annihilation. To calculate those fluxes we need to solve the propagation equation for the antiprotons [54, 113, 116–119]:

$$\nabla\cdot\left[K_0R^\delta\nabla\frac{\mathrm{d}n}{\mathrm{d}\varepsilon}\right] - \nabla\cdot\left[V_\mathrm{c}\frac{\mathrm{d}n}{\mathrm{d}\varepsilon}\right] - n^\mathrm{H}v_{\bar{p}}(\varepsilon)\sigma^\mathrm{in}_\mathrm{H}(\varepsilon)\frac{\mathrm{d}n}{d\varepsilon} + Q(\varepsilon,x) = 0\,, \qquad (13)$$

where R is the rigidity (momentum per unit of charge, $R = p/Z$), V_c the galactic wind velocity (generating convections), n^H is the interstellar hydrogen density number,

$v_{\bar{p}}$ the velocity of the antiproton and $\sigma_{\rm H}^{\rm in}$ is the inelastic antiproton–hydrogen cross section. We used the diffusion model [54] of the DarkSusy package with the diffusion–convection [116] option, and $\delta = 0.6$, $V_{\rm c} = 10\,{\rm km\,s}{-}1$, and $K_0 = 25 \times 10^{27}\,{\rm cm^2\,s^{-1}}$. Antiprotons propagate further than positrons; the resulting flux is consequently slightly more sensitive to the dark matter distribution in the galaxy, and especially in its central region. After the propagation, the antiproton flux can be written

$$\phi_{\bar{p}}(R_0, T) = b\langle\sigma v\rangle \sum_i \frac{{\rm d}N^i}{{\rm d}T} B^i \left(\frac{\rho_0}{m_\chi}\right)^2 C_{\rm prop}(T)\,, \tag{14}$$

where T is the $\bar{p}$ kinetic energy, $C_{\rm prop}(T)$ contains the propagation effect, and b is a boost factor resulting from the halo clumpiness ($b = 1$ in the case of a smooth profile). Experiments such as BESS and CAPRICE have measured the antiproton flux. Their signals can be fitted by an astrophysical background antiproton flux and are peaked at 1.76 GeV for an antiproton flux of $\sim 2 \times 10^{-6} \bar{p}\,{\rm cm^{-2}\,s^{-1}\,sr^{-1}}$. The measurement at 37.5 GeV seems to suggest an excess compared to the standard astrophysical models. We computed the antiproton fluxes from neutralino annihilation in those two energy bins and, following [18], we have considered the region where $\phi_{\bar{p}}(R_0, 1.76) > 2 \times 10^{-7} \bar{p}\,{\rm cm^{-2}\,s^{-1}\,sr^{-1}}$. We also checked that we never exceeded the experimental results from BESS and CAPRICE in those two energy bins.

3 Collider searches

3.1 Constraints

3.1.1 The mass spectrum constraints

We have calculated lower bounds for the SUSY particles and lightest Higgs boson masses (we excluded parameter values leading to tachyons in the squark and slepton sector). We applied the LEP2 lower bound on the lightest chargino mass $m_{\chi_1^+} > 103.5\,{\rm GeV}$ [120]. Typically, the most constraining bound arises from the lower bound on the lightest Higgs boson mass. In the decoupling regime ($m_A \gg M_Z$), valid everywhere in our parameter space, $m_h > 114.4\,{\rm GeV}$ [121–123]. It is well known that the theoretical prediction of the Higgs mass is very sensitive to the top mass. The radiative corrections used for calculating the Higgs mass are well described in [125]. In our analysis, we assume $m_t = 175\,{\rm GeV}$, but we also illustrate how our results are modified when the top mass varies within the interval (178 to 182 GeV) in Fig. 10b [124].

3.1.2 The $b \to s\gamma$ branching ratio

One observable process for which SUSY particle contributions might be large is the radiative flavor changing decay $b \to s\gamma$ [126–130]. In the standard model this decay is mediated by loops containing the charge 2/3 quarks and W-bosons. In SUSY theories additional contributions come from loops involving charginos and stops, or top quarks and charged Higgs bosons. The measurements of the inclusive decay $B \to X_s\gamma$ at CLEO [131] and BELLE [132] give tightly bounds for the branching ratio $b \to s\gamma$. The experimental value for the branching ratio of the process $b \to s\gamma$ is $(3.52 \pm 0.30 \times 10^{-4})$ [133]. Combining the theoretical errors [134] ($\pm 0.30 \times 10^{-4}$) coming from its prediction by adding the two uncertainties in quadrature, we obtain $2.33 \times 10^{-4} \leq {\rm BR}(b \to s\gamma) \leq 4.15 \times 10^{-4}$, at the 3σ level. Typically, the $b \to s\gamma$ is more important for $\mu < 0$, but it is also relevant for $\mu > 0$, particularly when $\tan\beta$ is large.

3.1.3 The anomalous moment of the muon

We have also taken into account the SUSY contributions to the anomalous magnetic moment of the muon, $\delta a_\mu = a_{\rm SUSY} - a_{\rm SM}$ [136–140]. We used in our analysis the recent experimental results [141], as well as the most recent theoretical calculations of the standard model contributions [142–144]. A discrepancy of about 2.7σ between experiment and theory is found when e^+e^- data are used to estimate $a_{\rm SM}$, leaving room for a SUSY contribution of $a_{\rm SUSY} = (25.2 \pm 9.2) \times 10^{-10}$, or, at the 2σ level, $6.8 < a^1_{\rm SUSY}0 < 43.6$. Such a contribution favors $\mu > 0$ and rather light sleptons and gauginos. However, this discrepancy is smaller if tau data are instead used to evaluate $a_{\rm SM}$. We therefore do not restrict the parameter space with the δa_μ constraint, but we show the relevant contour $a_{\rm SUSY} = 6.8 \times 10^{-10}$ instead.

3.1.4 The $B_{\rm s} \to \mu^+\mu^-$ branching ratio

Finally, we have considered the limit [145, 146] on the $B_s \to \mu^+\mu^-$ branching ratio [147–150]. The upper bound on this process, ${\rm B}(B_s \to \mu^+\mu^-) < 2.9 \times 10^{-7}$, does not constrain the parameter space of mSUGRA. However, it has been stressed recently that for non-universal soft terms the constraint can be large [151, 152], especially for large $\tan\beta$ and low Higgs masses. There is also a strong correlation between the $B_s \to \mu^+\mu^-$ branching ratio and cross sections for direct [152] and indirect [59] dark matter detection.

3.2 LHC

The LHC is a pp collider with a center of mass energy of $\sqrt{s}$ =14 TeV, expected to come on-line in 2007. Hadronic colliders produce mainly colored particles such as squark pairs $\tilde{q}\tilde{q}$, squark–antisquark pairs $\tilde{q}\tilde{q}^*$, gluino pairs $\tilde{g}\tilde{g}$ or associated squark–gluino pairs $\tilde{q}\tilde{g}$:

$$\begin{aligned} &q\overline{q},\ gg \to \tilde{q}\tilde{q}^*\,,\\ &qq \to \tilde{q}\tilde{q}\,,\\ &q\overline{q},\ gg \to \tilde{g}\tilde{g}\,,\\ &qg \to \tilde{q}\tilde{g}\,. \end{aligned}$$

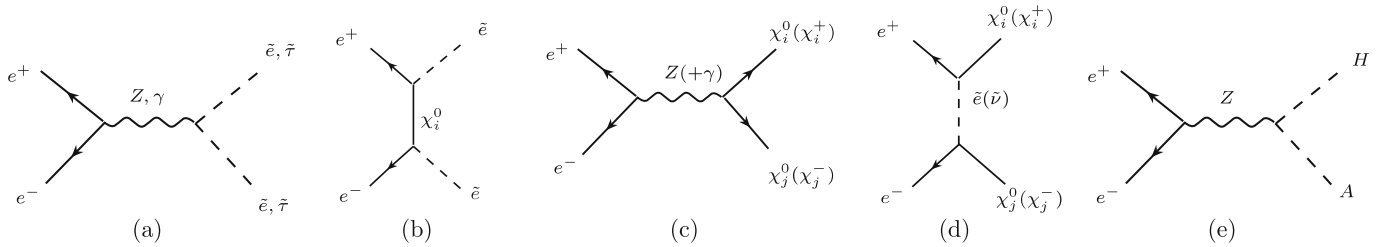

Fig. 3. Production processes for a linear collider

The $\tilde{q}\tilde{q}^*$ final state requires an initial state of the form $q\overline{q}$ or gg, whereas squark pairs are produced only from the qq state. Gluino pairs come from $q\overline{q}$ and gg states and the squark–gluino pairs are produced only via quark–gluon collisions. Cross sections for squark and gluino productions are very high at LHC, e.g. for $m_{\tilde{q}} = m_{\tilde{g}} = 500\,\mathrm{GeV}$, $\sigma(\tilde{q}-\tilde{g}) \sim 62\,\mathrm{pb}$. For an integrated luminosity of $100\,\mathrm{fb}^{-1}$, corresponding to one year of LHC data at high luminosity, 6.2×10^6 squark–gluino pairs are anticipated, leading to a promising (assuming that the detectors are well understood) discovery potential and to hints as to the underlying SUSY model. Of course, for a heavier spectrum, cross sections will be lower, but in any case, the production of squarks and gluinos at the LHC, if kinematically allowed, should be significant.

The decays of squarks and gluinos lead to multi-jets + isolated leptons + missing E_T signals. We consider the exclusion limits of [153–155], which establish that squarks and gluinos could be detected up to $m_{\tilde{q}\tilde{q}} \sim 2$–$2.5\,\mathrm{TeV}$ for the first two generations of squarks, which corresponds nearly to the parton–parton kinematic limit of roughly $14/3\,\mathrm{TeV}$. The detection of the third generation of squarks (sbottom, $\tilde{b}_1$ and stop, $\tilde{t}_1$) appears to be more difficult with a hadronic collider due to their special decay modes [156, 157].

3.3 Sparticle production in e^+e^- colliders

We also analyzed the prospects for producing SUSY particles and heavy Higgs bosons at high energy and high luminosity e^+e^- colliders [158–163]. In this exploratory study we assess the accessibility of certain production modes simply through the corresponding total cross section without performing any background studies. However, in most cases the clean experimental environment offered by e^+e^- colliders should allow for the discovery of a certain mode, given a sample of a few dozen events. Difficulties might arise in some narrow regions of parameter space, which we describe below. The proposed international linear collider (ILC) would operate at CM energies of around $\sqrt{s} \sim 0.5$–$1\,\mathrm{TeV}$, whereas the CERN CLIC linear collider is proposed to operate in the multi-TeV regime [164]. In our study, we have taken the example of a future linear collider with a center of mass energy of 1 TeV and an integrated luminosity of $500\,\mathrm{fb}^{-1}$. We will consider a given channel visible if its total cross section exceeds $\sigma_\mathrm{min} = 0.1\,\mathrm{fb}$, corresponding to 50 events per year.

In our study, we consider the following production processes, shown on Fig. 3:

$$
\begin{aligned}
&e^+e^- \to \tilde{l}\tilde{l}^* \quad (\text{mainly } \tilde{\tau}\tilde{\tau} \text{ and } \tilde{\nu}\tilde{\nu})\,,\\
&e^+e^- \to \chi^+\chi^-\,,\\
&e^+e^- \to \chi\chi_2^0\,,\\
&e^+e^- \to HA\,.
\end{aligned}
$$

Sleptons are produced in $\tilde{e}^\pm_\mathrm{R,L}$ pairs via the s-channel photon and Z-boson exchange and the t-channel exchange of the four neutralinos χ_i^0. Since the electron Yukawa coupling is suppressed, only the gaugino fraction of the neutralinos exchanged contributes to the process. Thus the influence of the soft breaking gaugino masses M_1, M_2 and μ through M_{H_u} is important in the production cross section, because they determine precisely the gaugino fraction of the neutralino. In particular, slepton pair production at next-generation e^+e^- colliders will be accessible if m_0 is not very large, away from the focus point region. The dominant final state is the lightest state, $\tilde{e}_\mathrm{R}$, and as in supergravity models, the $\tilde{e}_\mathrm{R}$–$\tilde{e}_\mathrm{L}$ mass difference may be large. For the third generation slepton, production proceeds only via γ and Z-boson exchange. In this case, we concentrate on the production of the lightest state, $e^+e^- \to \tilde{\tau}_1\tilde{\tau}_1$, which offers the largest discovery possibilities. The formulas in the appendix of [23, 24] indicate a strong dependence of the cross section on the selectron velocity β. Only sleptons with masses of several GeV below the kinematical limit can be observed.[3] Note that it is also possible to produce and observe sleptons through their decay even if $m_{\tilde{l}} > \sqrt{s}/2$ [165, 166].

Due to couplings and kinematics, the sleptons decay mainly into their leptonic partners and the gaugino-like neutralinos or charginos (if allowed). Whereas the lighter $\tilde{e}_\mathrm{R}$ decays predominantly through $\tilde{e}^\pm_\mathrm{R} \to e^\pm\chi_1^0$, the heavier left-handed $\tilde{e}_\mathrm{L}$ decays into the wino-like charginos $\chi_1^\pm$ or the neutralinos χ_2^0, because these processes occur via the SU(2) coupling, which is much stronger than the $\mathrm{U(1)_Y}$ involved in $\tilde{e}^\pm_\mathrm{R} \to e^\pm\chi_1^0$.

The charginos are produced through s-channel photon and Z-boson exchange as well as t-channel sneutrino exchange (see Fig. 3). Note that the sneutrino channel contributes with a sign [23, 24] opposite to the s-channel diagrams. The production is thus maximized in regions of

[3] We can also see it at the natural cross section suppression of spin 1 → spin 0 spin 0 processes.

heavy sneutrinos and for higgsino-like charginos ($|\mu| \ll M_2$). For a light sneutrino destructive interference can considerably diminish the cross section, whereas the production modes of higgsino-like charginos are largely insensitive to $m_{\tilde{\nu}}$ (the $\tilde{\nu}e\chi\pm_1$ coupling vanishes in this case). In any case, the cross section is usually rather large, making production possible for masses up to the kinematical threshold.

For $M_2, |\mu| <$ scalar/sleptons masses, the chargino is the lightest charged sparticle and decays mainly into $\chi_1^0 W$, with the W decaying into an ff' pair with a known branching ratio. For small slepton masses, virtual slepton exchange can enhance other processes leading to only $\tau^{\pm}\nu_{\tau}\chi_1^0$ final states [167, 168]. For large values of $\tan\beta$, a charged Higgs boson exchange contribution can also enhance the branching fraction for the τ final state.

The production of the lightest neutralinos $\chi_{1,2}^0$ occurs via s-channel Z-boson exchange and t- or u-channel $\tilde{e}_{\rm L}, \tilde{e}_{\rm R}$ exchanges. A gaugino-like neutralino does not couple to the Z-boson. However, a high higgsino fraction leads to enhancement of the $Z\chi_1^0\chi_2^0$ coupling and suppression of the $e\tilde{e}_{\rm L,R}\chi_{1,2}^0$ coupling proportional to the gaugino fraction of the neutralinos. Except in the extreme higgsino limit, the cross section is much smaller than the chargino cross section (whose nature ensures a reasonable production rate for gaugino-like of higgsino-like charginos through Z exchange).

The decay modes of the χ_2^0 depends strongly on the SUSY parameter space and can be completely leptonic (if the two-body decay $\chi_2^0 \to l^{\pm}\tilde{l}^{\mp}$ is the dominant process) or hadronic (if $\chi_2^0 \to h\chi_1^0$ is dominant). However, at an e^+e^- collider, hadronic χ_2^0 decays are as easy to observe as the leptonic decays. The only difficulty lies in regions of the parameter space where the mass difference $m_{\chi_2^0} - m_{\chi_1^0}$ is small, and where χ_2^0 decays almost exclusively into quasi-invisible modes.

If the pseudoscalar mass is sufficiently heavy (around 200 GeV, depending on $\tan\beta$) the model is in the so-called decoupling regime [169, 170, 172, 173], where the masses of the scalar H and the pseudoscalar A (and even $H^{\pm}$ for larger m_A) are almost degenerate. In this limit, both the (tree-level) coupling of the A and the H to massive vector bosons are suppressed, as well as the ZAh coupling. In this case, the only significant Higgs production process is the associated HA production through Z-boson exchange in the s-channel (see Fig. 3) [169, 170, 172, 173]. In any case, the cross section is suppressed by the kinematical β^3 factor near threshold.

If $m_A < 2m_t$ or $\tan^2\beta > m_t/m_b$, the heavy scalar Higgs boson H and pseudoscalar A decay predominantly into $b\overline{b}$ and $\tau\overline{\tau}$ pairs [169, 170, 172, 173]. If the $t\overline{t}$ channel is kinematically allowed and for lower values of $\tan\beta$, the process $A/H \to t\overline{t}$ dominates the decay modes. In some regions of the parameter space, decays into SUSY particles are possible. These modes will be more difficult to analyze in the framework of an e^+e^- collider, but the signals should be clear enough to be detectable [174–176].

We draw attention to the fact that we did not include initial state radiation in our calculation but we did verify its weak relative importance for the focus of the present work with regard e.g. to the astrophysical uncertainties.

4 Prospects for discovery

Using the theoretical, experimental, and cosmological constraints discussed in the previous sections, we perform a full scan of the $(m_0, m_{1/2})$ plane for a given value of $\tan\beta$ and A_0, fixing the higgsino parameter μ to be positive. The results are illustrated in Figs. 4–9, showing the regions allowed by the different constraints imposed in universal (Figs. 4 and 5), gaugino non-universal (Figs. 6 and 7), and scalar non-universal (Figs. 8 and 9) scenarios. We also delimit the regions of the parameter space that will become accessible in the near future for typical experiments of the different kinds of detection discussed above. The influence of the other external free parameters (m_t and galactic profiles) is illustrated in Fig. 10.

The areas excluded or disfavored by the experimental constraints are shown in grey. For the anomalous moment of the muon, the black dashed lines correspond to $\delta a_\mu = 6.8 \times 10^{10}$, which decreases in the direction of increasing m_0. The cosmologically favored relic density range $0.03 < \Omega_\chi \mathrm{h}^2 < 0.3$ is shown in yellow (very light grey) and the WMAP [5, 6] constraint, (1), is the internal black region inside the yellow (very light grey) area. Our starting parameter space is the universal mSUGRA/CMSSM plane, where one assumes a unified gaugino and scalar mass at the GUT scale ($m_{1/2}$ and m_0 respectively). We first choose $A_0 = 0$, $\tan\beta = 35$, $\mu > 0$ and perform a full scan of the $(m_0, m_{1/2})$ plane, where $0 < m_0 < 6000$ GeV and $0 < m_{1/2} < 2000$ GeV. We then examine the effects of non-universal mass terms in the gaugino and Higgs sectors (wino mass $M_2|_{\rm GUT}$, gluino mass $M_3|_{\rm GUT}$, up-type Higgs mass $M_{H_u}|_{\rm GUT}$ and down-type Higgs mass $M_{H_d}|_{\rm GUT}$) as well as $\tan\beta$ and m_t.

4.1 Universal case

For intermediate values of $\tan\beta$, two regions yield a neutralino relic abundance in agreement with $\Omega_{\rm CDM}h^2$ from WMAP. The first is at low m_0, where the lighter stau, $\tilde{\tau}_1$, is almost degenerate with the neutralino and where $\tilde{\tau}_1\chi$ and $\tilde{\tau}_1\tilde{\tau}_1$ coannihilations reduce the relic density sufficiently. The second region lies along the boundary where electroweak symmetry breaking cannot be achieved radiatively (hyperbolic branch/focus point (HB/FP): a high m_0 corresponding to a low μ). In this region the neutralino is a mixed bino–higgsino, enhancing $\chi\chi$ annihilation through Z exchange and $\chi\chi_1^+, \chi\chi_2^0$ coannihilations. These two regions are generically thin and fine tuned. Direct dark matter detection experiments are then favored for light Higgs scalar H (mainly low $m_0, m_{1/2}$) or around the HB/FP region where the higgsino fraction is sufficient to increase significantly the scattering cross section off nuclei and allow for detection in experiments such as ZEPLIN (see Fig. 4a).

For indirect detection with neutrino telescopes, a significant signal from the Sun requires a large higgsino fraction to enhance the spin dependent interaction $\chi q \xrightarrow{Z} \chi q$. This can occur only in the HB/FP branch where a km^3 size detector like ICECUBE will be able to probe models satisfying the WMAP constraint (see Fig. 4b).

Indirect gamma detection of neutralinos in the galactic center requires an efficient annihilation cross section.

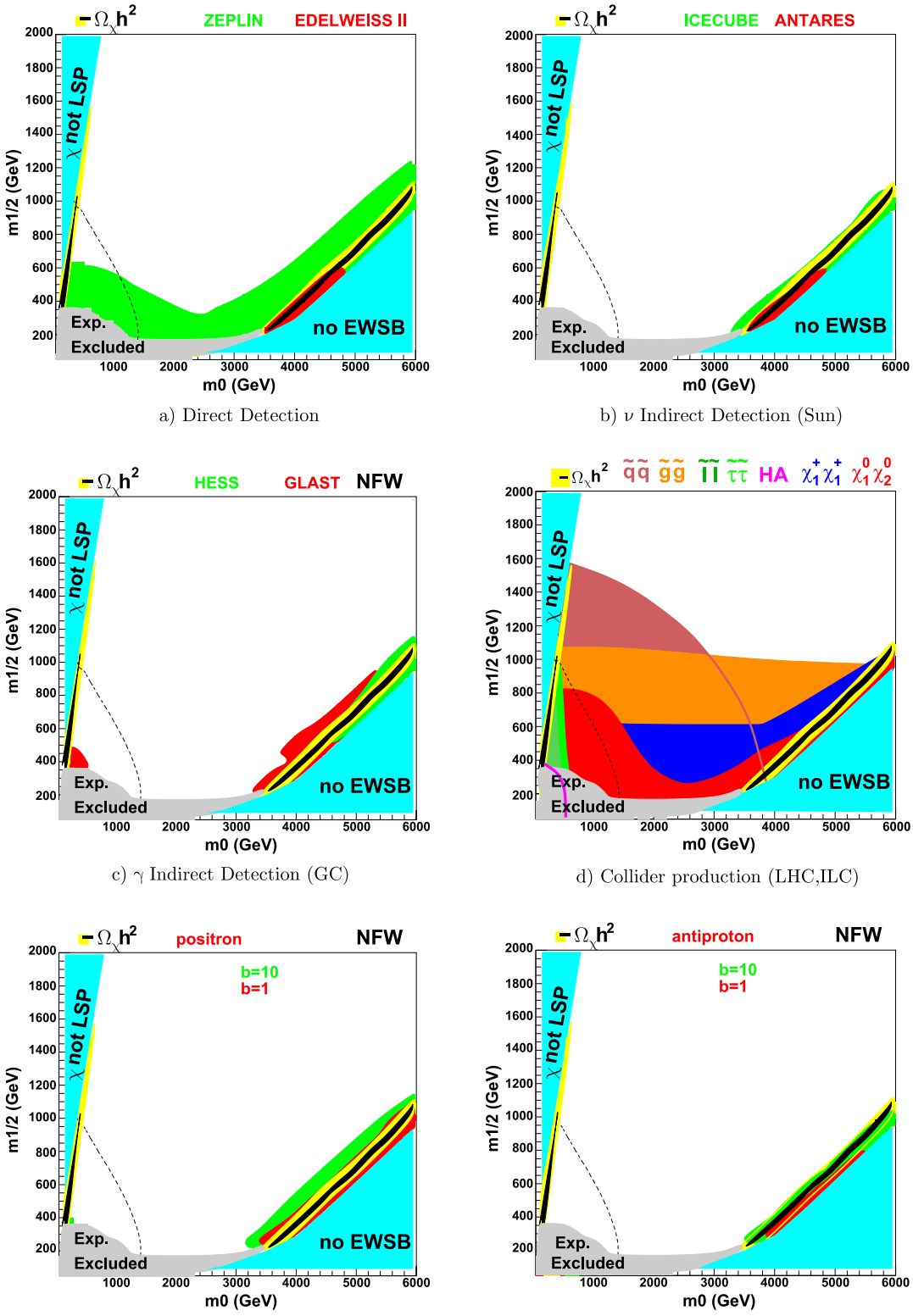

a) Direct Detection

b) ν Indirect Detection (Sun)

c) γ Indirect Detection (GC)

d) Collider production (LHC,ILC)

c) e^+ Indirect Detection (halo)

f) $\bar{p}$ Indirect Detection (halo)

Fig. 4. mSUGRA universal $A_0 = 0$, $\tan\beta = 35$, $\mu > 0$

One possible process is $\chi\chi \xrightarrow{A} b\bar{b}$, favored where the pseudoscalar A is light (low $m_0, m_{1/2}$), or when the $\chi\chi A$ coupling ($\propto z_{11(2)}z_{13(4)}$) is enhanced by the higgsino fraction in the HB/FP branch. Another annihilation process is $\chi\chi \xrightarrow{Z} t\bar{t}$, favored since the $\chi\chi Z$ coupling is proportional to $z^2_{13(4)}$. The opening of the $t\bar{t}$ annihilation process is clearly visible in Figs. 4c, 5c and 7c by a "bump" in the GLAST detection rate around $m_{1/2} \sim 400\,\text{GeV}$, corres-

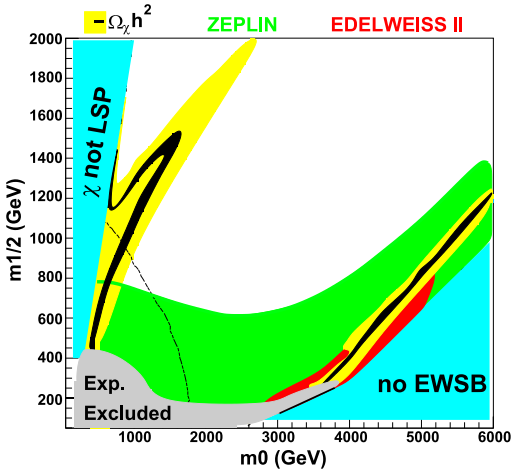

a) Direct Detection

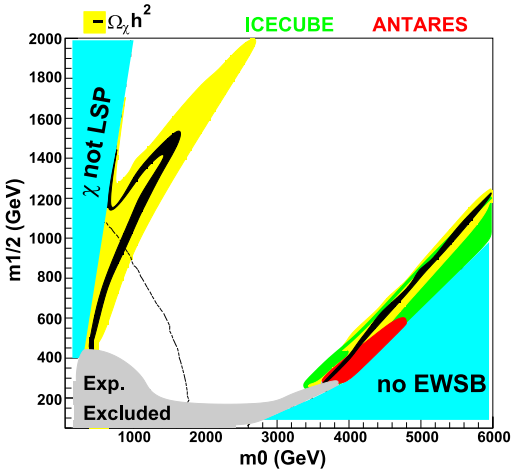

b) ν Indirect Detection (Sun)

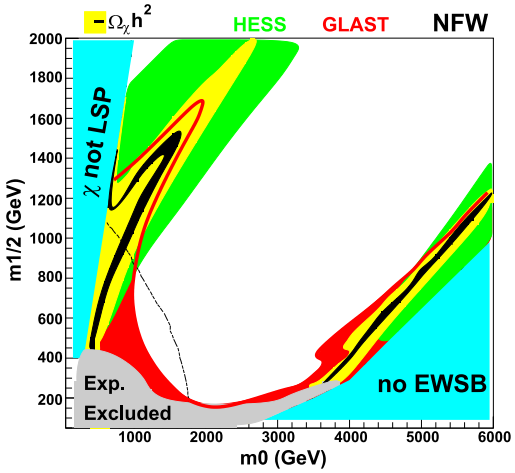

c) γ Indirect Detection (GC)

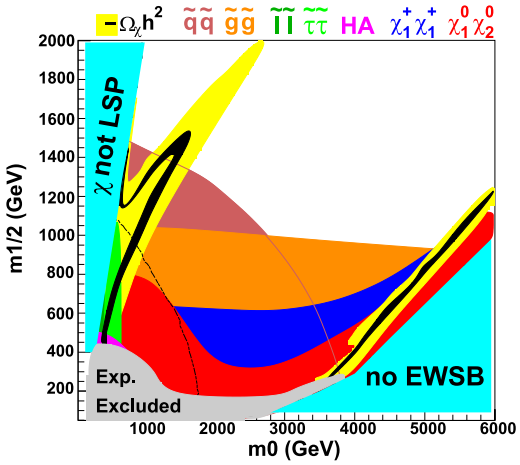

d) Collider production (LHC,ILC)

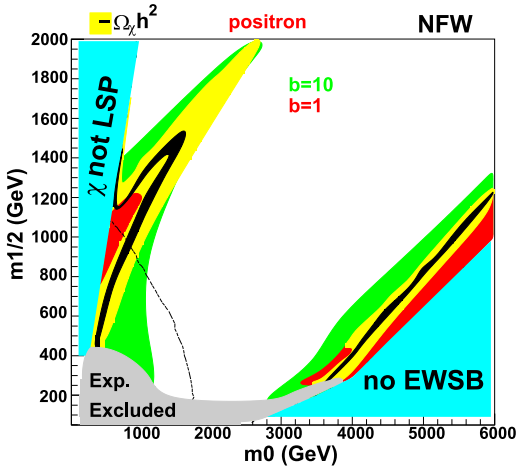

c) e^+ Indirect Detection (halo)

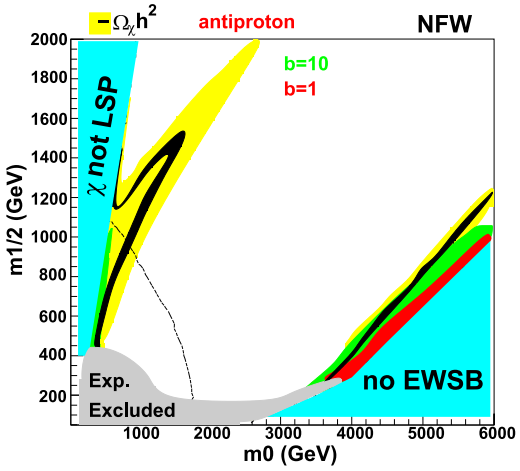

f) $\bar{p}$ Indirect Detection (halo)

Fig. 5. mSUGRA universal $A_0 = 0$, $\tan\beta = 50$, $\mu > 0$

ponding to a neutralino mass around200 GeV. This zone is within reach of the HESS telescope and will be covered by future satellites such as GLAST, as we can clearly see in Fig. 4c. This figure should be compared to 10c and 10d to emphasize the importance of the halo profile assumptions. The positron and antiproton fluxes have essentially the same particle physics dependence as the gamma-ray fluxes through the annihilation cross section factor $\langle \sigma v \rangle$.

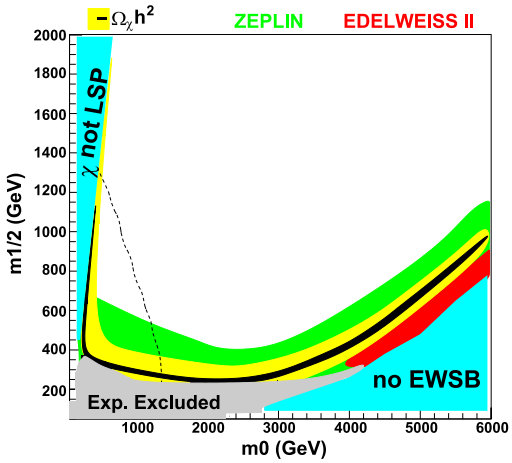

a) Direct Detection

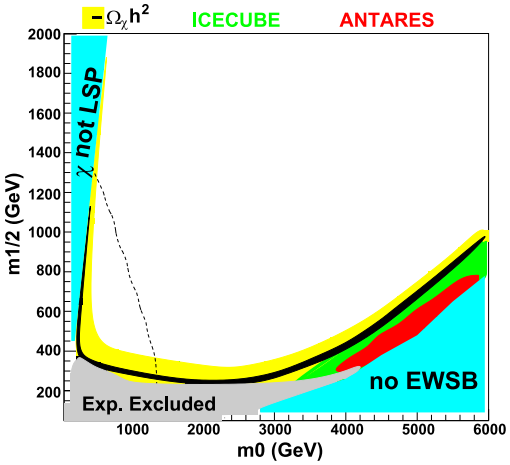

b) ν Indirect Detection (Sun)

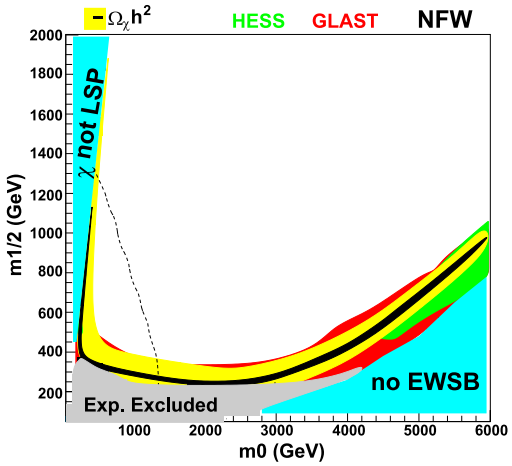

c) γ Indirect Detection (GC)

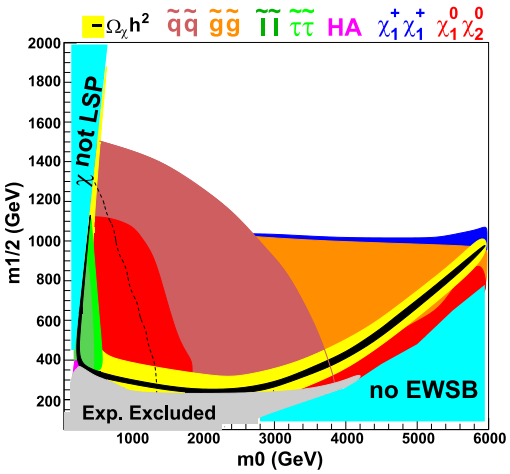

d) Collider production (LHC,ILC)

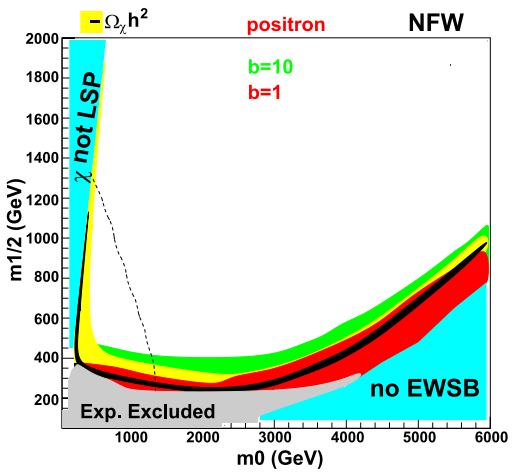

c) e^+ Indirect Detection (halo)

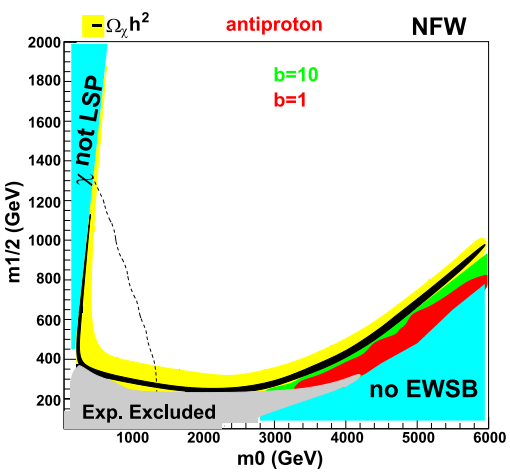

f) $\bar{p}$ Indirect Detection (halo)

Fig. 6. mSUGRA non-universal $M_2|_{\rm GUT} = 0.6$ $m_{1/2}$, $A_0 = 0$, $\tan\beta = 35$, $\mu > 0$

The favored region for positron and antiproton production is thus also located where the neutralino annihilation is strong, and an experiment similar to PAMELA should be able to detect any signal from this region for a sufficiently large boost factor (see 4e and 4f).

Prospects for producing SUSY particles and heavier Higgs bosons at future colliders are shown on Fig. 4d. The LHC will be efficient in the parameter space where the particles charged under SU(3) are light: light squarks $\tilde{q}$ ($m_0 \lesssim 2$–2.5 TeV) and/or light gluinos $\tilde{g}$ (small M_3, i.e., $m_{1/2} \lesssim$

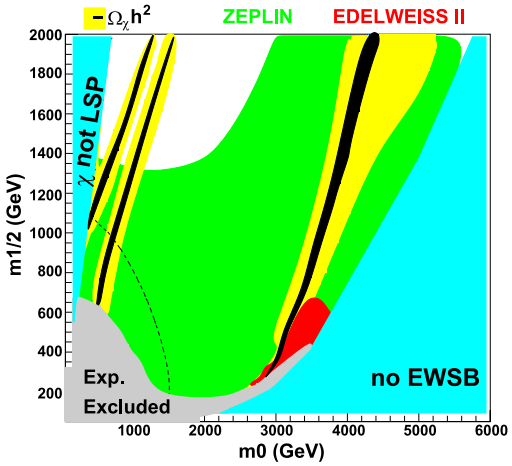

a) Direct Detection

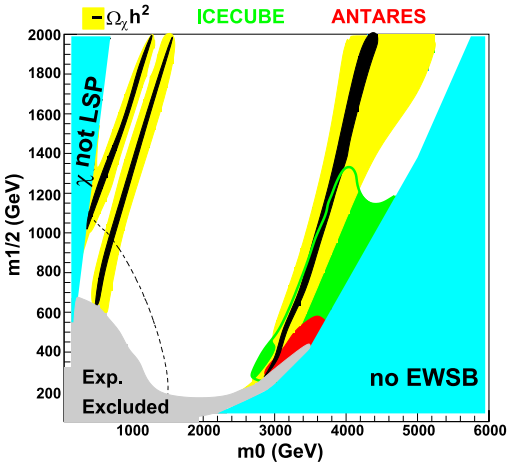

b) ν Indirect Detection (Sun)

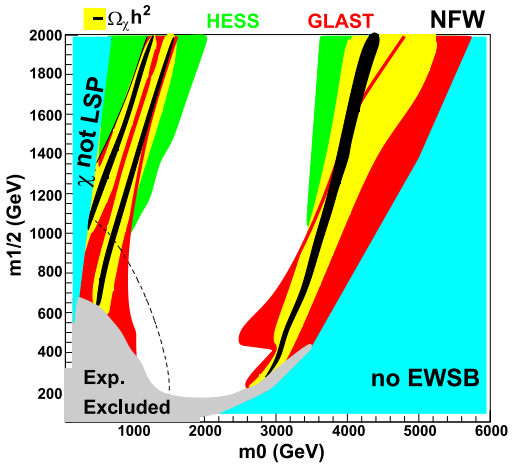

c) γ Indirect Detection (GC)

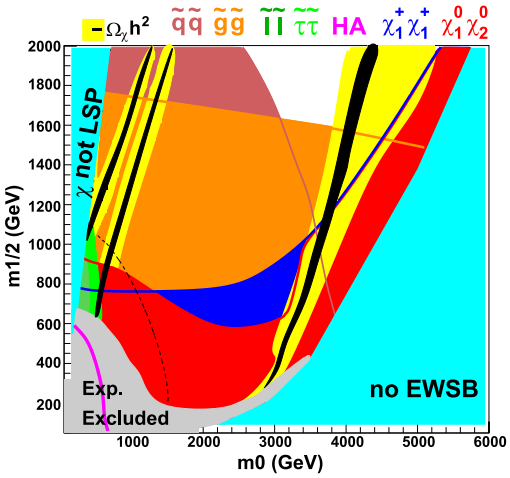

d) Collider production (LHC,ILC)

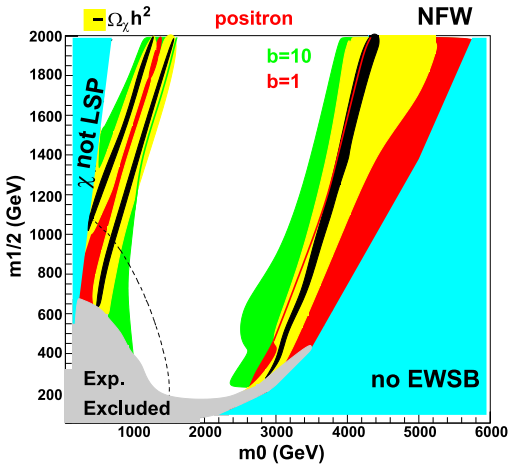

c) e^+ Indirect Detection (halo)

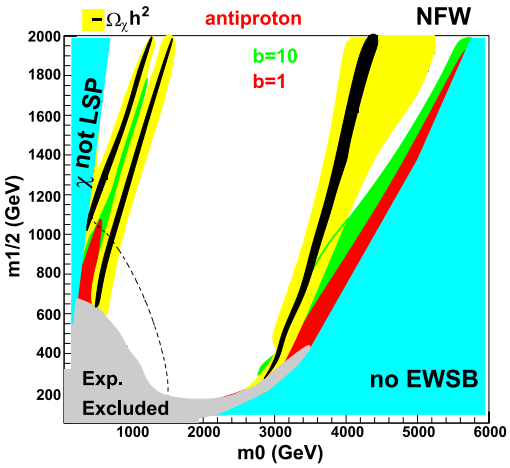

f) $\bar{p}$ Indirect Detection (halo)

Fig. 7. mSUGRA non-universal $M_3|_{\rm GUT} = 0.6$ $m_{1/2}$, $A_0 = 0$, $\tan\beta = 35$, $\mu > 0$

1000). A future 1 TeV linear collider can probe the slepton sector for light $\tilde{l}$ ($m_0 \lesssim 700$ GeV, $m_{1/2} \lesssim 1000$ GeV). $\chi\chi_2^0$ (mainly bino and wino, respectively) production is also favored for low m_0 through selectron exchange but decreases as $m_{\tilde{e}}$ (mainly m_0) increases up to $m_0 \sim 2000$ GeV, where the higgsino fraction of the neutralinos allows for Z exchange along the EWSB boundary. Chargino production follows first the kinematical limit of wino chargino production ($m_{1/2} \sim 600$ GeV, $2m_{\chi_1^+} \simeq 2 \times 0.8 \times m_{1/2} \simeq 1$ TeV) and then reaches higher $m_{1/2}$ values thanks to the higgsino

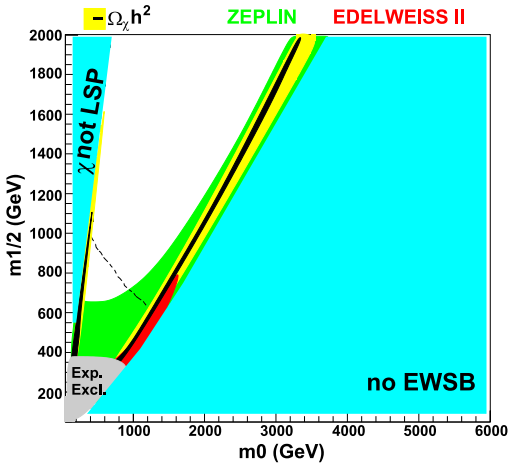

a) Direct Detection

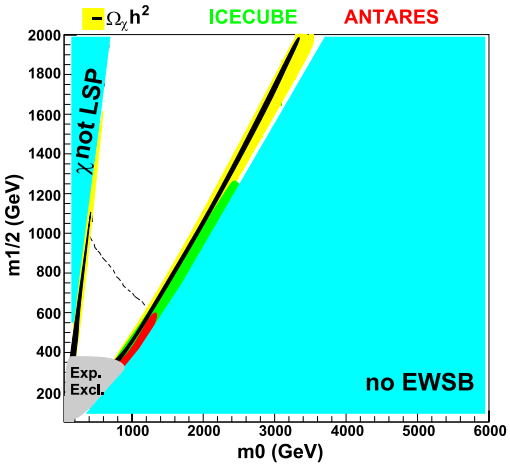

b) ν Indirect Detection (Sun)

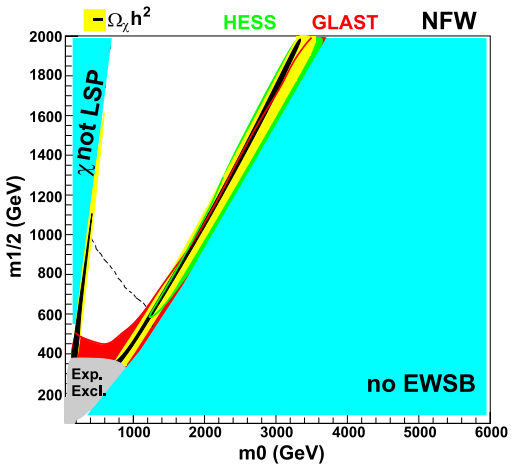

c) γ Indirect Detection (GC)

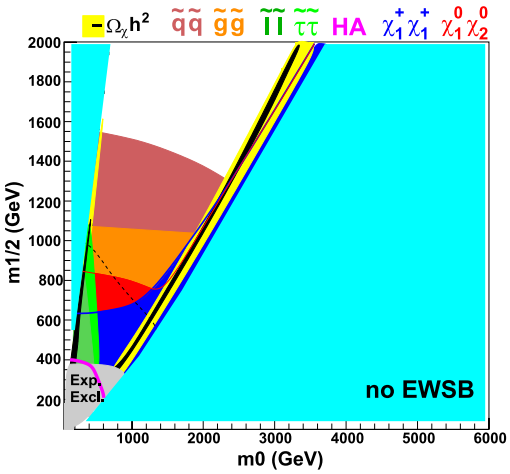

d) Collider production (LHC,ILC)

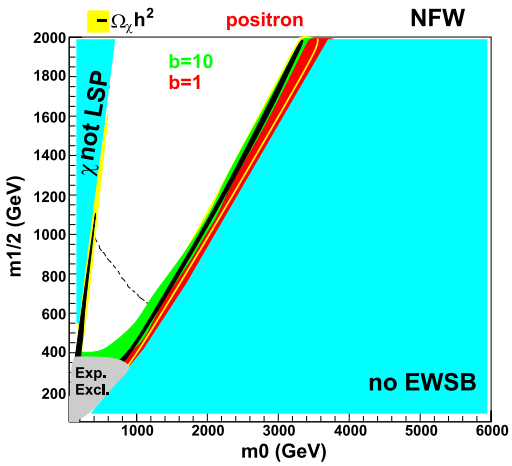

c) e^+ Indirect Detection (halo)

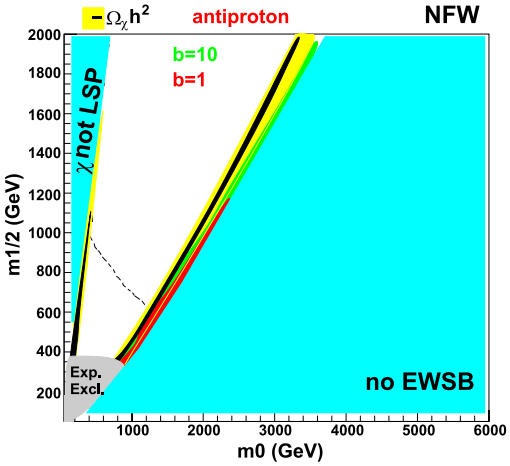

f) $\bar{p}$ Indirect Detection (halo)

Fig. 8. mSUGRA non-universal $M_{H_u}|_{\rm GUT} = 1.2m_0$

component of χ_1^+ along the EWSB boundary at high m_0. The region with a sufficiently copious HA production is restricted to the lower left corner of the plane and has already been excluded experimentally.

Non-zero values for the trilinear coupling A_0 term affect mainly third generation sfermion masses, which become split. Such a splitting is unimportant for dark matter searches like direct detection and indirect neutrino de-

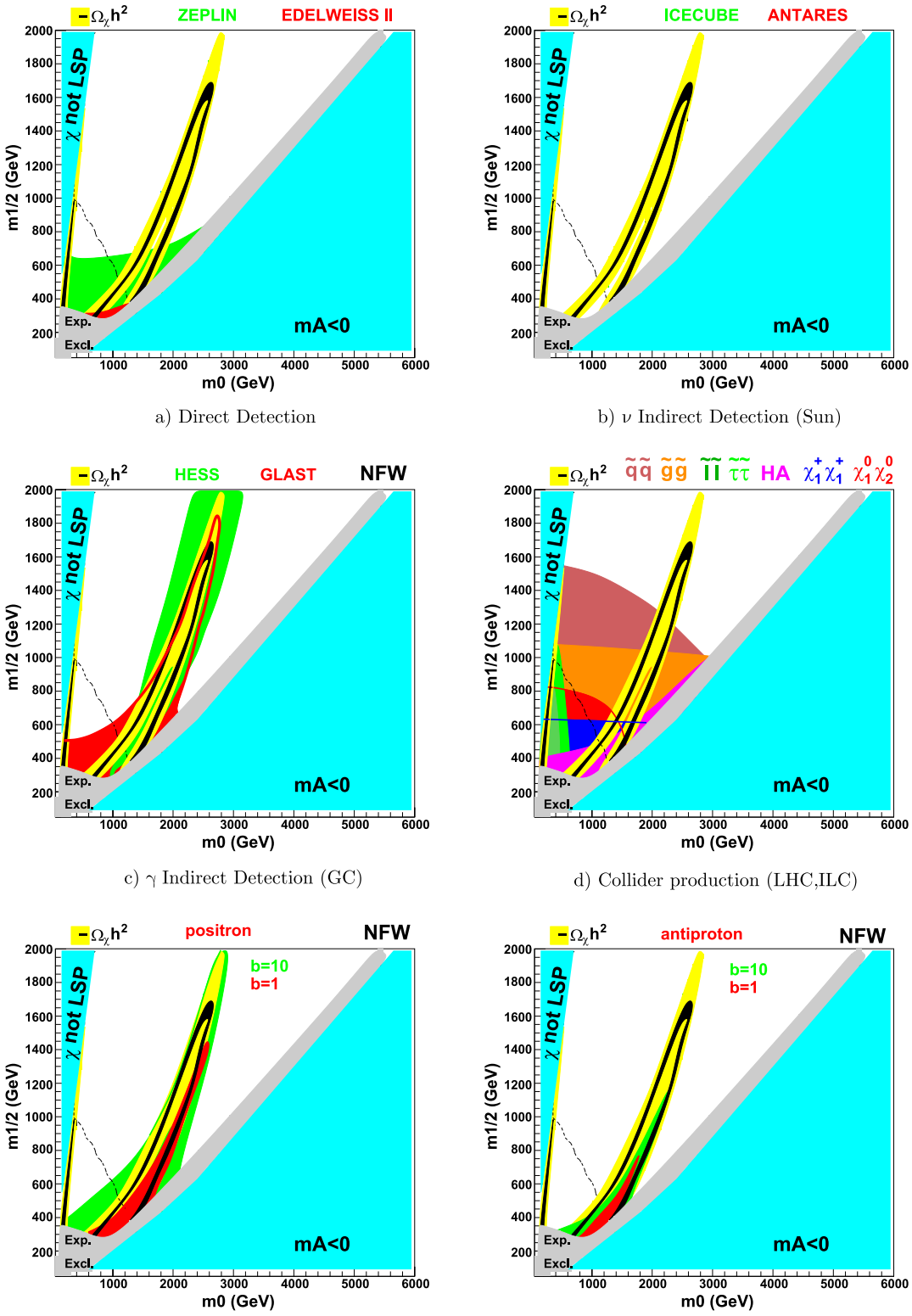

a) Direct Detection

b) ν Indirect Detection (Sun)

c) γ Indirect Detection (GC)

d) Collider production (LHC,ILC)

c) e^+ Indirect Detection (halo)

f) $\bar{p}$ Indirect Detection (halo)

Fig. 9. mSUGRA non-universal $M_{H_d}|_{\rm GUT} = 0.4m_0$

tection, which involve essentially first generation quark–squarks coupling from proton scattering. Annihilation can be enhanced by a positive non-zero value of the trilinear coupling through $\tilde{\tau}, \tilde{b}, \tilde{t}$ exchange, which may be of interest for indirect $\gamma, e^+, \bar{p}$ detection.

Non-zero trilinear couplings also favor $\chi\tilde{\tau}$ ($\chi\tilde{b}, \chi\tilde{t}$) coannihilations. The presence of such coannihilation channels leads to small cross sections for dark matter search experiments. However, the possibility exists to observe $\chi\tilde{\tau}$ coannihilation in regions of large dark matter density. In the extreme case, the $\chi\tilde{q}$ coannihilation region leads to a signal difficult to detect at LHC (essentially missing $E_{\rm T}$ and a few jets), but on the other hand the possibility of lighter squarks ($\tilde{b}$ or $\tilde{t}$) may favor LHC detection, especially in the low m_0 region. Such a trilinear mixing also favors the discovery at a 1 TeV linear collider through production of a lighter stau at low m_0. We should notice here also that $A_0 = m_0$ pushes away the focus point region.

The value of m_t strongly influences the existence and position of the focus point region, which strongly depends on the Yukawa coupling of the top quark. We show the relic density and collider detection capability for $m_t = 178$ and 182 GeV on Fig. 10a and 10b, respectively. For $m_t = 178$ GeV, one must extend the m_0 range up to 9 TeV to reach the no-EWSB boundary, but this does not suffice for $m_t = 182$ GeV, where this region can exist for even larger values of m_0 (around 20 TeV), re-opening the question of fine tuning. As a consequence, the range shown on Fig. 10b does not contain any region with interesting relic density.

High values of $\tan\beta$ (~ 50) lead to light Higgs bosons A, H, opening a Higgs funnel which decreases the relic density. This situation enhances annihilation and favors indirect $\gamma, e^+, \bar{p}$ detection. A lighter scalar Higgs boson H also increases the direct detection rate. A high $\tan\beta$ also enhances the splitting in the Isospin $= 1/2$ sfermion mass matrix, favoring LHC discovery, e.g. in the case of a lighter $\tilde{b}$ squark, whereas for a lighter stau, $\tilde{\tau}$, H, A favor their production in a linear collider, as it is clearly shown in Fig. 5.

4.2 Gaugino sector

4.2.1 The wino mass: $M_2|_{\rm GUT}$

We show in Fig. 6 the effects of the non-universality of the gaugino breaking mass term M_2. Other authors have al-

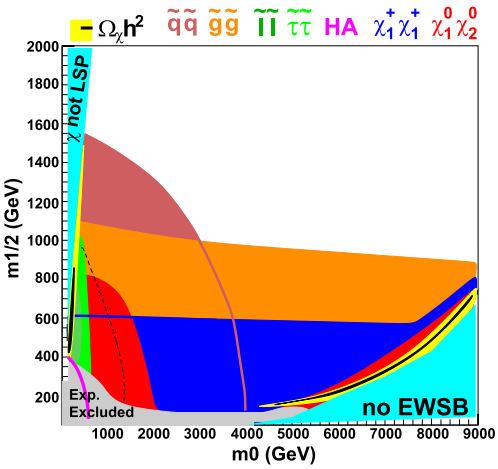

a) $m_t = 178$ GeV

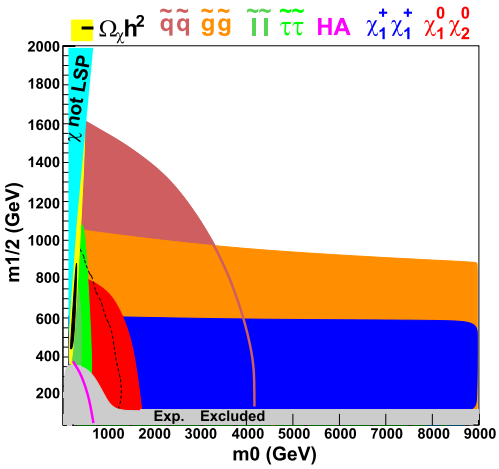

b) $m_t = 182$ GeV

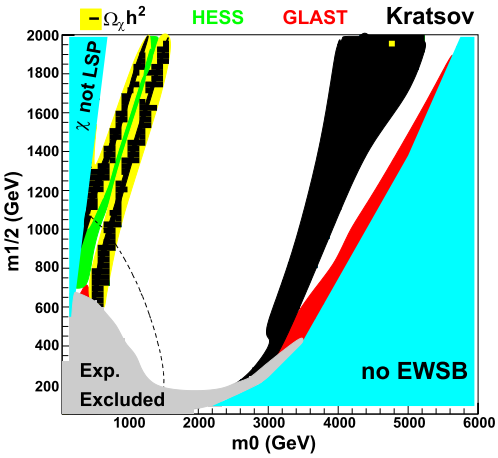

c) γ Indirect Detection : Kravtsov profile

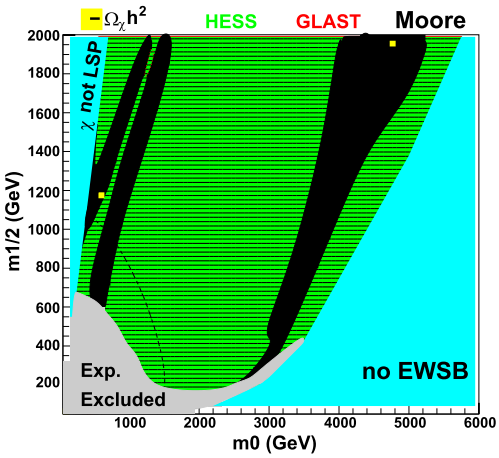

c) γ Indirect Detection : Moore profile

Fig. 10. Effect of $m_t = 178$ GeV in **a** and $m_t = 182$ GeV in **b** on LHC and ILC performances in the universal case (to be compared with Fig. 4d). Halo profile influence on indirect γ detection. $A_0 = 0$, $\tan\beta = 35$, $\mu > 0$ for non-universal gluino mass $M_3|_{\rm GUT} = 0.6 m_{1/2}$ with a Kravtsov profile in **c** and a Moore profile in **d** (to be compared with the NFW profile case Fig. 7c)

ready emphasized the phenomenological and cosmological effects of non-universality of the mass breaking terms [177–179]. Decreasing $M_2|_{\rm GUT}$ increases the wino content of the neutralino, which strongly decreases the relic density [31–33]. A near-WMAP value is obtained for an almost equal bino and wino amount, i.e. $M_1 \simeq M_2$ at the SUSY breaking scale, requiring $M_2 \simeq 0.6 m_{1/2}$ at the GUT scale [32]. Direct detection is favored through better couplings in the diffusion cross section (no $\tan\theta_W$ suppression of the bino coupling). Indirect gamma, positron, and antiproton detection is also facilitated by the large fluxes coming from strong annihilation, $\chi\chi \to W^+W^-$, when $m_\chi > m_W$, and the enhancement of the $\chi\chi A$ coupling for s-channel A exchange. For indirect neutrino detection, the wino component has no effect on capture in the Sun, but the annihilation can give a harder neutrino spectrum from W^+W^- decays. The situation at LHC is the same as for the universal case. The linear collider detection prospects are very good because of the lighter neutralino and chargino through their wino component. The $\chi\chi_2^0, \chi^+\chi^-$ can thus be produced for higher values of $m_{1/2}$. A smaller $M_2/m_{1/2}$ ratio at the GUT scale can lead to $\chi\chi_1^+$ and $\chi\chi_2^0$ degeneracies, which can affect the detection procedure. It is important to keep in mind that the numerical computation of Ωh^2 is very sensitive to the wino fraction in χ. Detection prospects are thus poor in regions of parameter space satisfying the WMAP constraints, with low M_2 at the GUT scale. We show in Fig. 6 the results for $M_2/m_{1/2} = 0.6$ at the GUT scale, but we mention that for $M_2/m_{1/2} = 0.55$ the whole $(m_0, m_{1/2})$ plane has $\Omega_\chi h^2 < 0.1$, but the regions accessible to dark matter experiments correspond to regions where the relic density is too low ($\Omega_\chi h^2 < 0.03$). One must increase $m_{1/2}(m_\chi)$ to obtain a relic density satisfying the WMAP constraints with a smaller $M_2/m_{1/2}$ ratio.

4.2.2 The gluino mass: $M_3|_{\rm GUT}$

Figure 7 shows the effects of non-universality of the gaugino mass breaking term M_3. The gluino mass parameter considerably influences the MSSM spectrum through the renormalization group equations (see for instance [12] for a review of the subject). Decreasing M_3 decreases the squark masses and increases the up-type Higgs mass $M_{H_u}^2$ at low energy, where it becomes less negative, and decreases the down-type Higgs mass $M_{H_d}^2$, which implies a smaller $m_{\rm A,H}$ and an increase of the higgsino content of neutralinos and charginos. That can easily be understood looking at the approximate tree-level relations:

$$\mu^2 \simeq -M_{H_u}^2 - 1/2 M_Z^2 \quad \text{and} \quad m_A^2 \simeq M_{H_d}^2 - M_{H_u}^2 - M_Z^2 \,. \tag{15}$$

As a result, now relic density constraints are more easily satisfied than in the universal case: both $\chi\chi \xrightarrow{A} b\bar{b}$ annihilation (higher coupling and lighter A, which can open the A funnel) is enhanced and the focus point region with the $\chi\chi \xrightarrow{Z} t\bar{t}$ annihilation process is enlarged. Direct detection benefits from higher $z_{11}z_{13}$ couplings and a lighter scalar Higgs boson H. The higher higgsino fraction favors indirect neutrino detection through the coupling in $\chi q \xrightarrow{Z} \chi q$ of the capture rate. Gamma, positron, and indirect antiproton detection is favored by the annihilation enhancement. LHC gets a strong potentiality enhancement because the squarks (especially the $\tilde{t}_1$) and gluinos are lighter than in the universal case. Finally, HA production at a 1 TeV linear collider is kinematically enhanced, H and A being lighter than in mSUGRA. $\chi^+\chi^-$ $\chi\chi_2^0$ production is also favored, because of a lower value for μ. As in the non-universal wino mass case, smaller $M_3|_{\rm GUT}/m_{1/2}$ values can lead to $\chi\chi_1^+$ and $\chi\chi_2^0$ degeneracies, now through the higgsino component, which impedes detection, but those regions have a too small relic density, decimated by coannihilation, to be viable. These points are illustrated in Fig. 7 for the ratio $M_3/m_{1/2} = 0.6$ at the GUT scale [32]. Such models with a light gluino are very interesting for SUSY detection and all neutralino dark matter detection techniques and can be found in some effective string inspired scenarios [36–39].

4.3 Higgs sector

4.3.1 Up-type Higgs mass: $M_{H_u}|_{\rm GUT}$

Figure 8 shows the detection prospects for $M_{u_cH}/m_0 = 1.2$ at the GUT scale. Increasing the up-type Higgs mass M_{H_u} at the GUT scale has some effects common with the case described above, where the gluino mass is decreased, as can explicitly be seen from (15). One notes that the sensitivity on this parameter is high, leading to a thinner allowed region with interesting results and a "no-EWSB" area wider compared to the previous non-universal gluino mass case. As for the gaugino sector [32] we varied non-universal parameters in the Higgs sector at the GUT scale (M_{H_u}/m_0 and M_{H_d}/m_0) and found for the up-type mass that the value of the ratio leading to a WMAP relic density is around 1.2 for $\tan\beta = 35$. For the universal case, the mixed bino–higgsino region is larger, but the pseudoscalar Higgs A is still too heavy to open the on-shell A-pole channel. All kinds of dark matter detection are thus possible in the resulting mixed bino–higgsino region. In this region, for a future linear collider, chargino production is copious, and some HA pairs are also produced. Squark and gluino production at the LHC is not enhanced, but LHC detection is possible over a large part of the non-excluded region of parameter space.

4.3.2 Down-type Higgs mass: $M_{H_d}|_{\rm GUT}$

Figure 9 illustrates the case of non-universality $M_{H_d}/m_0 = 0.4$ at the GUT scale. Indeed, the ratio $M_{H_d}/m_0 < 1$ can have interesting phenomenological consequences for the different detection rates. By decreasing the down-type Higgs mass, M_{H_d}, at the GUT scale, one essentially decreases $m_{A,H}$, as can be seen in (15). The excluded region at high values of m_0 results from the negative mass of the pseudoscalar as well as from the absence of EWSB. The A-pole can open more easily, providing a corridor with the correct relic density within the WMAP bounds. In this corridor, neutralino annihilation is large,

facilitating discovery through indirect γ, e^+ and $\bar{p}$ detection. The low value of m_{H_d} gives also significant direct detection rates, but one must keep in mind that the neutralino is almost exclusively bino in the whole remaining region of the $(m_0, m_{1/2})$ plane where the $\chi\chi H$ coupling is suppressed. Because of a small higgsino fraction, neutrino telescopes are ineffective for those kinds of models. The LHC has a discovery potential similar to that of mSUGRA, but the allowed models cover a wider area of the parameter space. Only the Higgs production HA is enhanced at the Linear Collider compared to the universal case, while gaugino–higgsino neutralino and chargino production is suppressed.

5 Summary and conclusion

Dark matter experiments and collider searches will provide stringent tests of low energy supersymmetry and neutralino dark matter models within the framework of the minimal supersymmetric standard model. The possible correlations between (or absence of) signals of different kinds of detection impose impressive constraints on the models and scenarios both for supersymmetry theory and astrophysics.

We summarize the links between the different possibilities to fulfill the WMAP dark matter density constraint, the parameters involved, and the most promising detection techniques.

The $\chi\tilde{\tau}(\tilde{t})$ coannihilation region typically has a small cross section for dark matter detection. This is for huge direct detection experiments if $m_{\tilde{\tau}}$ and m_h are correlated (low $m_{\tilde{\tau}}$ to favor the coannihilation process and light H to favor direct detection scattering) as well as for indirect γ detection in the case of a favorable galactic profile (with a stronger cusp than in the NFW profile). The LHC may be of interest through $\tilde{q}\tilde{q}$ if $m_{\tilde{q}}$ is correlated to $m_{\tilde{l}}$ and the ILC through $\tilde{\tau}\tilde{\tau}$ to probe the $\tilde{\tau}$ coannihilation region.

The Higgs funnel region $\chi\chi \xrightarrow{A} b\bar{b}(\tau\bar{\tau})$ of parameter space is enlarged compared to the universal case for non-universal M_3 or M_{H_u} or M_{H_d}. Direct detection benefits from a large cross section. However, coupling enhanced by a neutralino with a large higgsino component is required to compensate for the large value of m_A. Indirect γ $(e^+, \bar{p})$ detection is facilitated by this annihilation process. However, the constraints obtained depend sensitively on the astrophysics hypotheses. The LHC detection prospects depend on $m_{\tilde{q},\tilde{g}}$ compared to m_A, and for the ILC, $\chi\chi_2^0$ and HA production is favored up to the energy threshold.

The hyperbolic branch/focus point with mixed bino–higgsino χ at high m_0 values and especially non-universal M_3 or M_{H_u} parameters is the more promising region for the DM searches. Direct detection can provide constraints on the nature of the neutralino by correlations between spin dependent/independent experiments as well as through correlations with a neutrino telescope. Indirect $\gamma(e^+, \bar{p})$ detection of γ, e^+ or $\bar{p}$ is favored through the enhancement of annihilation processes. Moreover, this mixed neutralino region is the only one accessible to neutrino telescopes for a signal coming from the Sun (a km^3 size telescope will probe up to $m_\chi \sim 600\,\mathrm{GeV}$). The chargino production in an e^+e^- collider as well as gluino production for LHC are the relevant processes, but they are suppressed at very high values of the mass breaking terms, where moreover $\delta_\mu^{\mathrm{SUSY}} = 0$.

Finally a mixed bino–wino χ is very sensitive to a non-universal M_2 parameter. The wino component enhances the dark matter rates (Ωh^2 is very sensitive to the wino fraction). The LHC signal is significant if the gluino mass is correlated to the wino mass and wino-like neutralino/chargino production in ILC is possible up to $m_{\chi(\chi_1^+)} \simeq 500\,\mathrm{GeV}$.

However, even if a part of the supersymmetric spectrum is discovered at LHC, it will be difficult to measure precisely the properties of the particles entering in the relic density computation. Consequently, both types of data (astroparticle and accelerator physics) will be required to extract more complete information on the underlying model.

Whereas the focus point (FP) region characterized by heavy scalars will be more easily probed by dark matter searches due to the nature of the neutralino, the region with a heavy gaugino and light sfermions will be more accessible to collider experiments. Since dark matter signals give little information on the nature of the dark matter, and since new physics collider signals are not easily linked to dark matter signals, it will be crucial to combine both astrophysical and accelerator data to constrain any supersymmetric extension of the standard model (deeper information on both supersymmetry and the nature of the dark matter sector can thus be obtained by correlation of the different signals or by absence of a signal).

Acknowledgements. Work by E.N. is supported by the I.I.S.N. and the Belgian Federal Science Policy (return grant and IAP 5/27). Y.M. wants to warmly thank P. Zerwas for sharing his incredible knowledge and enthusiasm and the DESY theory group for their scientific and financial support. The authors are grateful to M. Bucher, A. Djouadi, J. B. De Vivie and the referee for their advice, corrections and update during the writing of this work.

References

1. G. Bertone, D. Hooper, J. Silk, Phys. Rep. **405**, 279 (2005) [arXiv:hep-ph/0404175]
2. G. Jungman, M. Kamionkowski, K. Griest, Phys. Rep. **267**, 195 (1996) [arXiv:hep-ph/9506380]
3. K. Olive, arXiv:astro-ph/0301505 *Summary of lectures given at the Theoretical Advanced Study Institute in Elementary Particle Physics at the University of Colorado at Boulder, June 2–28, 2002*, and references therein
4. C. Muñoz, Int. J. Mod. Phys. A **19**, 3093 (2004) [arXiv:hep-ph/0309346]
5. C.L. Bennett et al., Astrophys. J. **148**, 1 (2003) [arXiv: astro-ph/0302207]
6. D.N. Spergel et al., Astrophys. J. **148**, 175 (2003) [arXiv: astro-ph/0302209]

7. J.A. Tauber, Astrophys. Lett. Comm. **37**, 145 (2000)
8. K. Freese, B.D. Fields, D.S. Graff, arXiv:astro-ph/0002058
9. P. Fayet, S. Ferrara, Phys. Rep. **32**, 249 (1977)
10. H.E. Haber, G.L. Kane, Phys. Rep. **117**, 75 (1985)
11. R. Barbieri, Riv. Nuovo Cimento **11N4**, 1 (1988)
12. S.P. Martin, arXiv:hep-ph/9709356
13. B.C. Allanach, G. Belanger, F. Boudjema, A. Pukhov, JHEP **0412**, 020 (2004) [arXiv:hep-ph/0410091]
14. A. Djouadi, J.L. Kneur, G. Moultaka, arXiv:hep-ph/0211331; see also the web page http://www.lpm.univ-montp2.fr:6714/~kneur/suspect.html
15. G. Belanger, F. Boudjema, A. Pukhov, A. Semenov, Comput. Phys. Commun. **149**, 103 (2002) [arXiv:hep-ph/0112278]
16. G. Belanger, F. Boudjema, A. Pukhov, A.G. Semenov, "MicrOMEGAs: Version 1.3" arXiv:hep-ph/0405253; see also the web page http://wwwlapp.in2p3.fr/lapth/micromegas
17. P. Gondolo, J. Edsjo, P. Ullio, L. Bergstrom, M. Schelke, E.A. Baltz, JCAP **0407**, 008 (2004) [arXiv:astro-ph/0406204]; http://www.physto.se/ edsjo/darksusy/
18. H. Baer, A. Mustafayev, S. Profumo, A. Belyaev, X. Tata, arXiv:hep-ph/0504001
19. H. Baer, A. Mustafayev, E.K. Park, S. Profumo, arXiv:hep-ph/0505227
20. J.R. Ellis, T. Falk, G. Ganis, K.A. Olive, M. Srednicki, Phys. Lett. B **510**, 236 (2001)
21. J.R. Ellis, K.A. Olive, Y. Santoso, New J. Phys. **4**, 32 (2002)
22. L. Roszkowski, R. Ruiz de Austri, T. Nihei, JHEP **0108**, 024 (2001)
23. A. Djouadi, M. Drees, J.L. Kneur, JHEP **0108**, 055 (2001)
24. H. Baer, C. Balazs, A. Belyaev, JHEP **0203**, 042 (2002)
25. J. Ellis, A. Ferstl, K.A. Olive, Y. Santoso, arXiv:hep-ph/0302032
26. J.L. Feng, K.T. Matchev, F. Wilczek, Phys. Rev. D **63**, 045 024 (2001) [arXiv:astro-ph/0008115]
27. U. Chattopadhyay, A. Corsetti, P. Nath, arXiv:hep-ph/0303201
28. J. Ellis, K.A. Olive, Y. Santoso, V.C. Spanos, arXiv:hep-ph/0303043
29. V. Berezinsky, A. Bottino, J. Ellis, N. Fornengo, G. Mignola, S. Scopel, Astropart. Phys. **5**, 1 (1996) [arXiv:hep-ph/9508249]
30. P. Nath, R. Arnowitt, Phys. Rev. D **56**, 2820 (1997) [arXiv:hep-ph/9701301]
31. A. Birkedal-Hansen, B.D. Nelson, Phys. Rev. D **64**, 015 008 (2001) [arXiv:hep-ph/0102075]
32. V. Bertin, E. Nezri, J. Orloff, JHEP **02**, 046 (2003) [arXiv:hep-ph/0210034]
33. A. Birkedal-Hansen, B.D. Nelson, Phys. Rev. D **67**, 095 006 (2003) [arXiv:hep-ph/0211071]
34. D.G. Cerdeno, E. Gabrielli, M.E. Gomez, C. Munoz, JHEP **0306**, 030 (2003) [arXiv:hep-ph/0304115]
35. D.G. Cerdeno, C. Munoz, JHEP **0410**, 015 (2004) [arXiv:hep-ph/0405057]
36. P. Binetruy, Y. Mambrini, E. Nezri, Astropart. Phys. **22**, 1 (2004) [arXiv:hep-ph/0312155]
37. G. Bertone, P. Binetruy, Y. Mambrini, E. Nezri, arXiv:hep-ph/0406083
38. P. Binetruy, A. Birkedal-Hansen, Y. Mambrini, B.D. Nelson, arXiv:hep-ph/0308047
39. A. Falkowski, O. Lebedev, Y. Mambrini, arXiv:hep-ph/0507110
40. A. Corsetti, P. Nath, Phys. Rev. D **64**, 125 010 (2001) [arXiv:hep-ph/0003186]
41. S. Profumo, Phys. Rev. D **68**, 015 006 (2003)
42. P. Ullio, Nucl. Phys. Proc. Suppl. **110**, 82 (2002)
43. A. Cesarini, F. Fucito, A. Lionetto, A. Morselli, P. Ullio, arXiv:astro-ph/0305075
44. D. Hooper, L.T. Wang, Phys. Rev. D **69**, 035 001 (2004) [arXiv:hep-ph/0309036]
45. D.G. Cerdeno, C. Munoz, Phys. Rev. D **66**, 115 007 (2002) [arXiv:hep-ph/0206299]
46. A. Bottino, F. Donato, N. Fornengo, S. Scopel, arXiv:hep-ph/0401186
47. F. Donato, N. Fornengo, D. Maurin, P. Salati, Phys. Rev. D **69**, 063 501 (2004) [arXiv:astro-ph/0306207]
48. A.B. Lahanas, N.E. Mavromatos, D.V. Nanopoulos, Int. J. Mod. Phys. D **12**, 1529 (2003) [arXiv:hep-ph/0308251]
49. J. Edsjo, M. Schelke, P. Ullio, P. Gondolo, JCAP **0304**, 001 (2003) [arXiv:hep-ph/0301106]
50. E.A. Baltz, J. Edsjo, Phys. Rev. D **59**, 023 511 (1999) [arXiv:astro-ph/9808243]
51. D. Hooper, J. Silk, Phys. Rev. D **71**, 083 503 (2005) [arXiv:hep-ph/0409104]
52. D. Hooper, J.E. Taylor, J. Silk, Phys. Rev. D **69**, 103 509 (2004) [arXiv:hep-ph/0312076]
53. E.A. Baltz, J. Edsjo, K. Freese, P. Gondolo, Phys. Rev. D **65**, 063 511 (2002) [arXiv:astro-ph/0109318]
54. L. Bergstrom, J. Edsjo, P. Ullio, APJ **526**, 215 (1999) [arXiv:astro-ph/9902012]
55. P. Ullio, L. Bergstrom, J. Edsjo, C.G. Lacey, Phys. Rev. D **66**, 123 502 (2002) [arXiv:astro-ph/0207125]
56. Y. Mambrini, C. Munoz, arXiv:hep-ph/0407158
57. Y. Mambrini, C. Munoz, JCAP **0410**, 003 (2004) [arXiv:hep-ph/0407352]
58. S. Baek, Y.G. Kim, P. Ko, JHEP **0502**, 067 (2005) [arXiv:hep-ph/0406033]
59. Y. Mambrini, C. Munoz, E. Nezri, F. Prada, arXiv:hep-ph/0506204
60. W. de Boer, M. Herold, C. Sander, V. Zhukov, A.V. Gladyshev, D.I. Kazakov, arXiv:astro-ph/0408272
61. G. Belanger, S. Kraml, A. Pukhov, arXiv:hep-ph/0502079
62. G. Belanger, F. Boudjema, A. Cottrant, A. Pukhov, A. Semenov, arXiv:hep-ph/0412309
63. G. Belanger, F. Boudjema, A. Cottrant, A. Pukhov, A. Semenov, Nucl. Phys. B **706**, 411 (2005) [arXiv:hep-ph/0407218]
64. R. Arnowitt, B. Dutta, T. Kamon, V. Khotilovich, arXiv:hep-ph/0411102
65. L.S. Stark, P. Hafliger, A. Biland, F. Pauss, arXiv:hep-ph/0502197
66. H. Baer, A. Belyaev, T. Krupovnickas, J. O'Farrill, JCAP **0408**, 005 (2004) [arXiv:hep-ph/0405210]
67. G.R. Blumenthal, S.M. Faber, R. Flores, J.R. Primack, Astrophys. J. **301**, 27 (1986)
68. J. Edsjo, M. Schelke, P. Ullio, arXiv:astro-ph/0405414
69. F. Prada, A. Klypin, J. Flix, M. Martinez, E. Simonneau, Phys. Rev. Lett. **93**, 241 301 (2004)
70. O.Y. Gnedin, A.V. Kravtsov, A.A. Klypin, D. Nagai, Astrophys. J. **616**, 16 (2004) [arXiv:astro-ph/0406247]
71. P. Gondolo, J. Silk, Phys. Rev. Lett. **83**, 1719 (1999) [arXiv:astro-ph/9906391]

72. D. Merrit, Phys. Rev. Lett. **92**, 201 304 (2004)
73. M.W. Goodman, E. Witten, Phys. Rev. D **31**, 3059 (1985)
74. A. Djouadi, M. Drees, Phys. Lett. **B484**, 183 (2000)
75. The EDELWEISS Collaboration, V. Sanglard et al., arXiv:astro-ph/0503265
76. The CDMS Collaboration, R. Abusaidi et al., Phys. Rev. Lett. **84**, 5699 (2000)
77. The CDMS Collaboration, R. Abusaidi et al., Phys. Rev. D **66**, 122 003 (2002)
78. The DAMA Collaboration, R. Bernabei, Phys. Lett. B **480**, 23 (2000)
79. G. Chardin. Edelweiss dark matter search, talk given at the school and workshop on neutrino particle astrophysics, Les Houches, 21 January–1 February (2002)
80. The ZEPLIN Collaboration, R. Luscher et al., talk given the XXXVIIIth Rencontres de Moriond ELECTROWEAK INTERACTIONS AND UNIFIED THEORIES, 15–22 March 2003, Les Arcs, France
81. L. Brink et al., arXiv:astro-ph/0503583
82. M.S. Turner, Phys. Rev. D **34**, 1921 (1986)
83. L. Bergstrom, P. Ullio, J.H. Buckley, Astropart. Phys. **9**, 137 (1998) [arXiv:astro-ph/9712318]
84. J.F. Navarro, C.S. Frenk, S.D.M. White, Astrophys. J. **490**, 493 (1997)
85. B. Moore, T. Quinn, F. Governato, J. Stadel, G. Lake, arXiv:astro-ph/9903164
86. A.V. Kravtsov, A.A. Klypin, J.S. Bullock, J.R. Primack, arXiv:astro-ph/9708176
87. P. Jean et al., Astron. Astrophys. **407**, L55 (2003) [arXiv: astro-ph/0309484]
88. The EGRET Collaboration, S.D. Hunger et al., Astrophys. J. **481**, 205 (1997)
89. H.A. Mayer-Hasselwander et al., Astron. Astrophys. **335**, 161 (1998)
90. The VERITAS Collaboration, K. Kosack et al., Astrophys. J. **608**, L97 (2004) [arXiv:astro-ph/0403422]
91. The CANGAROO-II Collaboration, K. Tsuchiya et al., Astrophys. J. **606**, L115 (2004) [arXiv:astro-ph/0403592]
92. The HESS Collaboration, F. Aharonian et al., arXiv:astro-ph/0408145
93. C. Boehm, D. Hooper, J. Silk, M. Casse, J. Paul, Phys. Rev. Lett. **92**, 101 301 (2004) [arXiv:astro-ph/0309686]
94. M. Casse, B. Cordier, J. Paul, S. Schanne, Astrophys. J. **602**, L17 (2004) [arXiv:astro-ph/0309824]
95. G. Bertone, A. Kusenko, S. Palomares-Ruiz, S. Pascoli, D. Semikoz, arXiv:astro-ph/0405005
96. D. Hooper, B.L. Dingus, Phys. Rev. D **70**, 113 007 (2004) [arXiv:astro-ph/0210617]
97. The HESS Collaboration, J.A. Hinton et al., New Astron. Rev. **48**, 331 (2004) [arXiv:astro-ph/0403052]
98. N. Gehrels, P. Michelson, Astropart. Phys. **11**, 277 (1999); see also the web page http://www-glast.stanford.edu
99. The GLAST Collabortation, A. Morselli, A. Lionetto, A. Cesarini, F. Fucito, P. Ullio, arXiv:astro-ph/0211327
100. K. Griest, D. Seckel, Nucl. Phys. B **283**, 681 (1987)
101. K. Griest, D. Seckel, Nucl. Phys. B **296**, 1034 (1988) [Erratum]
102. A. Gould, Astrophys. J. **321**, 571 (1987)
103. V. Bertin, E. Nezri, J. Orloff, Eur. Phys. J. C **26**, 111 (2002) [arXiv:hep-ph/0204135]
104. G. Bertone, E. Nezri, J. Orloff, J. Silk, arXiv:astro-ph/0403322
105. T. Montaruli, Search for wimps using upward-going muons in macro, proceeedings of the 26th icrc in Salt Lake City 17–25 August (1999), pp. 277–280 [hep-ex/9905021]
106. O. Suvorova, Status and perspectives of indirect search for dark matter, published in Tegernsee 1999, Beyond the desert (1999), pp. 853–867
107. A. Habig. An indirect search for WIMPs with Super-Kamiokande, contributed to 27th ICRC, Hamburg, Germany, 7–15 August (2001)
108. http://amanda.uci.edu
109. http://antares.in2p3.fr
110. http://icecube.wisc.edu
111. D. Bailey, Ph.D. thesis (2002), http://antares.in2p3.fr/Publications/thesis/2002/d-bailey-thesis.ps.gz
112. J. Edsjo. Swedish astroparticle physics, talk given at the conference 'Partikeldagarna', Uppsala, Sweden, March 6 (2001)
113. I.V. Moskalenko, A.W. Strong, S.G. Mashnik, J.F. Ormes, Astrophys. J. **586**, 1050 (2003) [arXiv:astro-ph/0210480]
114. M. S. Longair, High-Energy Astrophysics (Cambridge, University Press, 1994)
115. The HEAT Collaboration, S.W. Barwick et al., Astrophys. J. **482**, L191 (1997) [arXiv:astro-ph/9703192]
116. I.V. Moskalenko, A.W. Strong, J.F. Ormes, M.S. Potgieter, Astrophys. J. **565**, 280 (2002) [arXiv:astro-ph/0106567]
117. D. Maurin, F. Donato, R. Taillet, P. Salati, Astrophys. J. **555**, 585 (2001) [arXiv:astro-ph/0101231]
118. D. Maurin, R. Taillet, F. Donato, Astron. Astrophys. **394**, 1039 (2002) [arXiv:astro-ph/0206286]
119. A.M. Lionetto, A. Morselli, V. Zdravkovic, arXiv:astro-ph/0502406
120. The ALEPH Collabortation, A. Heister et al., Phys. Lett. B **533**, 223 (2002)
121. The ALEPH Collabortation, R. Barate et al., Phys. Lett. B **565**, 61 (2003) [arXiv:hep-ex/0306033]
122. LEP Higgs Working Group, *Searches for the Neutral Higgs Bosons of the MSSM*, LHWG Note/2001-04, arXiv:hep-ex/0107030
123. LEP Higgs Working Group, *Search for the standard model Higgs boson at LEP*, LHWG Note/2002-01
124. The D0 Collaboration, V.M. Abazov et al., Nature **429**, 638 (2004) [arXiv:hep-ex/0406031]
125. B.C. Allanach, A. Djouadi, J.L. Kneur, W. Porod, P. Slavich, JHEP **0409**, 044 (2004) [arXiv:hep-ph/0406166]
126. S. Bertolini, F. Borzumati, A. Masiero, G. Ridolfi, Nucl. Phys. B **353**, 591 (1991)
127. R. Barbieri, G.F. Giudice, Phys. Lett. B **309**, 86 (1993) [arXiv:hep-ph/9303270]
128. F.M. Borzumati, Z. Phys. C **63**, 291 (1994) [arXiv:hep-ph/9310212]
129. The CLEO Collaboration, M.S. Alam et al., Phys. Rev. Lett. **74**, 2885 (1995)
130. G. Degrassi, P. Gambino, G.F. Giudice, JHEP **0012**, 009 (2000) [arXiv:hep-ph/0009337]
131. The CLEO Collaboration, S. Chen et al., Phys. Rev. Lett. **87**, 251 807 (2001) [arXiv:hep-ex/0108032]
132. The BELLE Collaboration, H. Tajima, Int. J. Mod. Phys. **A17**, 2967 (2002) [arXiv:hep-ex/0111037]
133. The Heavy Flavour Averaging Group Collaboration, http://www.slac.stanford.edu/xorg/hfag

134. P. Gambino, U. Haisch, M. Misiak, Phys. Rev. Lett. **94**, 061 803 (2005) [arXiv:hep-ph/0410155]
135. A. Djouadi, M. Drees, J.L. Kneur, arXiv:hep-ph/0504090
136. J.R. Ellis, J.S. Hagelin, D.V. Nanopoulos, Phys. Lett. B **116**, 283 (1982)
137. J.A. Grifols, A. Mendez, Phys. Rev. D **26**, 1809 (1982)
138. R. Barbieri, L. Maiani, Phys. Lett. B **117**, 203 (1982)
139. D.A. Kosower, L.M. Krauss, N. Sakai, Phys. Lett. B **133**, 305 (1983)
140. G. Degrassi, G.F. Giudice, Phys. Rev. D **58**, 053 007 (1998) [arXiv:hep-ph/9803384]
141. The Muon g-2 Collaboration, G.W. Bennett et al., Phys. Rev. Lett. **92**, 161 802 (2004) [arXiv:hep-ex/0401008]
142. M. Davier, S. Eidelman, A. Hocker, Z. Zhang, Eur. Phys. J. C **31**, 503 (2003) [arXiv:hep-ph/0308213]
143. K. Hagiwara, A.D. Martin, D. Nomura, T. Teubner, Phys. Rev. D **69**, 093 003 (2004) [arXiv:hep-ph/0312250]
144. J.F. de Troconiz, F.J. Yndurain, arXiv:hep-ph/0402285
145. The CDF Collaboration, D. Acosta et al., Phys. Rev. Lett. **93**, 032 001 (2004) [arXiv:hep-ex/0403032]
146. The D0 Collaboration, V.M. Abazov et al., Phys. Rev. Lett. **94**, 071 802 (2005) [arXiv:hep-ex/0410039]
147. K.S. Babu, C.F. Kolda, Phys. Rev. Lett. **84**, 228 (2000) [arXiv:hep-ph/9909476]
148. G. Isidori, A. Retico, JHEP **0111**, 001 (2001) [arXiv:hep-ph/0110121]
149. A. Dedes, H.K. Dreiner, U. Nierste, Phys. Rev. Lett. **87**, 251 804 (2001) [arXiv:hep-ph/0108037]
150. G. Isidori, A. Retico, J. High Energ. Phys. **0209**, 063 (2002) [arXiv:hep-ph/0110121]
151. S. Baek, Y.G. Kim, P. Ko, J. High Energ. Phys. **02**, 067 (2005) [arXiv:hep-ph/0406033]
152. S. Baek, D.G. Cerdeño, Y.G. Kim, P. Ko, C. Muñoz, J. High Energ. Phys. **06**, 017 (2005) [arXiv:hep-ph/0505019]
153. F. Charles, in: *Proc. of the 5th International Symposium on Radiative Corrections (RADCOR 2000)* ed. by Howard E. Haber [arXiv:hep-ph/0105026]
154. S. Abdullin, F. Charles, Nucl. Phys. B **547**, 60 (1999) [arXiv:hep-ph/9811402]
155. The CMS Collaboration, S. Abdullin et al., J. Phys. G **28**, 469 (2002) [arXiv:hep-ph/9806366]
156. C. Boehm, A. Djouadi, Y. Mambrini, Phys. Rev. D **61**, 095 006 (2000) [arXiv:hep-ph/9907428]
157. A. Djouadi, Y. Mambrini, Phys. Rev. D **63**, 115 005 (2001) [arXiv:hep-ph/0011364]
158. J.L. Feng, M.E. Peskin, H. Murayama, X. Tata, Phys. Rev. D **52**, 1418 (1995) [arXiv:hep-ph/9502260]
159. H. Murayama, M.E. Peskin, Ann. Rev. Nucl. Part. Sci. **46**, 533 (1996) [arXiv:hep-ex/9606003]
160. H. Baer, R. Munroe, X. Tata, Phys. Rev. D **54**, 6735 (1996)
161. H. Baer, R. Munroe, X. Tata, Phys. Rev. D **56**, 4424 (1997) [Erratum] [arXiv:hep-ph/9606325]
162. The ECFA/DESY LC Physics Working Group Collaboration, E. Accomando et al., Phys. Rep. **299** 1 (1998) [arXiv:hep-ph/9705442]
163. S. Dawson, M. Oreglia, Ann. Rev. Nucl. Part. Sci. **54**, 269 (2004) [arXiv:hep-ph/0403015]
164. The LHC/LC Study Group, G. Weiglein et al., Phys. Rep. **426**, 47 (2006) [arXiv:hep-ph/0410364]
165. A. Datta, A. Djouadi, M. Muhlleitner, Eur. Phys. J. C **25**, 539 (2002) [arXiv:hep-ph/0204354]
166. A. Datta, A. Djouadi, Eur. Phys. J. C **25**, 523 (2002) [arXiv:hep-ph/0111466]
167. A. Djouadi, Y. Mambrini, M. Muhlleitner, Eur. Phys. J. C **20**, 563 (2001) [arXiv:hep-ph/0104115]
168. A. Djouadi, Y. Mambrini, Phys. Lett. B **493**, 120 (2000) [arXiv:hep-ph/0007174]
169. A. Djouadi, J. Kalinowski, P.M. Zerwas, Z. Phys. C **70**, 435 (1996) [arXiv:hep-ph/9511342]
170. A. Djouadi, M. Spira, P.M. Zerwas, Z. Phys. C **70**, 427 (1996) [arXiv:hep-ph/9511344]
171. A. Djouadi, J. Kalinowski, M. Spira, Comput. Phys. Commun. **108**, 56 (1998) [arXiv:hep-ph/9704448]
172. A. Djouadi, arXiv:hep-ph/0503172
173. A. Djouadi, arXiv:hep-ph/0503173
174. A. Djouadi, J. Kalinowski, P.M. Zerwas, Z. Phys. C **57**, 569 (1993)
175. A. Djouadi, P. Ohmann, P.M. Zerwas, J. Kalinowski, arXiv:hep-ph/9605437
176. A. Djouadi, J. Kalinowski, P. Ohmann, P.M. Zerwas, Z. Phys. C **74**, 93 (1997) [arXiv:hep-ph/9605339]
177. J.R. Ellis, A. Ferstl, K.A. Olive, Y. Santoso, Phys. Rev. D **67**, 123 502 (2003) [arXiv:hep-ph/0302032]
178. U. Chattopadhyay, D.P. Roy, Phys. Rev. D **68**, 033 010 (2003) [arXiv:hep-ph/0304108]
179. H. Baer, C. Balazs, A. Belyaev, J. O'Farrill, arXiv:hep-ph/0305191